BAMS Article

The Flexible Array of Radars and Mesonets (FARM)

Joshua Wurman, Karen Kosiba, Brian Pereira, Paul Robinson, Andrew Frambach, Alycia Gilliland, Trevor White, Josh Aikins, Robert J. Trapp, Stephen Nesbitt, Maiana N. Hanshaw, and Jon Lutz

ABSTRACT: The Flexible Array of Radars and Mesonets (FARM) Facility is an extensive mobile/quickly deployable (MQD) multiple-Doppler radar and in situ instrumentation network. The FARM includes four radars: two 3-cm dual polarization, dual frequency (DPDF), Doppler on Wheels (DOW6/DOW7), the Rapid-Scan DOW (RSDOW), and a quickly deployable (QD) DPDF 5-cm C band on Wheels (COW). The FARM includes three mobile mesonet (MM) vehicles with 3.5-m masts, an array of rugged QD weather stations (PODNET), QD weather stations deployed on infrastructure such as light/power poles (POLENET), four disdrometers, six MQD upper-air sounding systems and a Mobile Operations and Repair Center (MORC). The FARM serves a wide variety of research/educational uses. Components have deployed to >30 projects during 1995–2020 in the United States, Europe, and South America, obtaining pioneering observations of a myriad of small spatial- and temporal-scale phenomena including tornadoes, hurricanes, lake-effect snow storms, aircraft-affecting turbulence, convection initiation, microbursts, intense precipitation, boundary layer structures and evolution, airborne hazardous substances, coastal storms, wildfires and wildfire suppression efforts, weather modification effects, and mountain/alpine winds and precipitation. The radars and other FARM systems support innovative educational efforts, deploying >40 times to universities/colleges, providing hands-on access to cutting-edge instrumentation for their students. The FARM provides integrated multiple radar, mesonet, sounding, and related capabilities enabling diverse and robust coordinated sampling of three-dimensional vector winds, precipitation, and thermodynamics increasingly central to a wide range of mesoscale research. Planned innovations include S-band on Wheels Network (SOWNET) and Bistatic Adaptable Radar Network (BARN), offering more qualitative improvements to the field project observational paradigm, providing broad, flexible, and inexpensive 10-cm radar coverage and vector wind field measurements.

KEYWORDS: Mesoscale processes; In situ atmospheric observations; Radars/Radar observations; Radiosonde/rawinsonde observations; Surface observations; Weather radar signal processing

https://doi.org/10.1175/BAMS-D-20-0285.1
Corresponding author: Joshua Wurman, jwurman@illinois.edu
Supplemental material: https://doi.org/10.1175/BAMS-D-20-0285.2

In final form 5 April 2021
©2021 American Meteorological Society
For information regarding reuse of this content and general copyright information, consult the AMS Copyright Policy.

Unauthenticated | Downloaded 02/01/24 06:03 PM UTC

AFFILIATIONS: Wurman, Kosiba, Pereira, Robinson, Frambach, Gilliland, White, Aikins, Trapp, and Nesbitt—University of Illinois at Urbana–Champaign, Champaign, Illinois; **Hanshaw**—CoreLogic, Boulder, Colorado; **Lutz**—Boulder, Colorado

This paper describes the Flexible Array of Mesonets and Radars (FARM) facility. The FARM is an extensive array of mobile and quickly deployable (MQD) radars, mobile mesonets, quickly deployable (QD) weather stations, sounding systems, and disdrometers providing a single source of diverse observational capabilities for research and education. The history, key achievements, capabilities, and future plans for FARM are described.

Why mobile/quickly deployable targeted radar arrays?

Value of radar observations. Narrow-beam, quickly scanning, meteorological radars have revolutionized the ability of scientists and forecasters to observe the atmosphere. Research and operational radars measure three-dimensional (3D) distributions of radial velocity and precipitation, typically updating every few minutes. A cursory review of the scientific literature reveals the seminal role of radars in research and operational meteorology dating back decades (e.g., Marshall and Palmer 1948; Stout and Huff 1953; Fujita 1965; Houze et al. 1990; Atlas 1990; Kumjian and Ryzhkov 2008). Many articles using data from radars appear in the refereed literature every month in any of several primary meteorological journals, focusing on scientific advances, forecasting, modeling, and technology. Specialized American Meteorological Society and European radar meteorology conferences focus primarily on radars and their applications. Many colleges and universities offer courses, and there are at least several textbooks (Doviak and Zrnić 1984; Rinehart 1990; Bringi and Chandrasekar 2001; Fabry 2015; Rauber and Nesbitt 2018) dedicated to, or with substantial focus on, radar meteorology. Radars are one of the core technologies used to guide hazardous weather warnings.

Limitations of stationary radars.

- Near-ground visibility: Some phenomena exhibit significant variations near the ground, below typical radar observing horizons. These include tornadoes (e.g., Bluestein and Golden 1993; Wurman et al. 1996, 2007c; Kosiba and Wurman 2013), microbursts (e.g., Fujita 1981; Wilson et al. 1984), snowbands (e.g., Niziol et al. 1995; Steiger et al. 2013), boundary layer fine lines (Wilson and Schreiber 1986; Marquis et al. 2007), hurricane boundary layer rolls (Wurman and Winslow 1998), and wind farm effects (Toth et al. 2011). These near-ground variations are invisible to operational radars such as the Next Generation Weather Radar (NEXRAD) network of Weather Surveillance Radar-1988 Doppler [WSR-88D; Office of the Federal Coordinator for Meteorological Services and Supporting Research (OFCM); OFCM 2017], with only ~1% of the NEXRAD observational domain observed below 200 m above radar level (ARL).
- Spatial scales: Many of these same high-impact phenomena exhibit spatial scales that are too small to observe regularly, or adequately resolve, given the spacing of typical operational radar networks.
- Temporal scales: Finally, many of these same phenomena evolve over very short time scales (Wurman et al. 2007a, 2013a, 2014), much shorter than the 120–300-s volumetric update rate of WSR-88Ds, and faster than even the quicker update rates of most research radars (Wurman and Randall 2001).

Spatial and temporal limitations of radar observations are illustrated in Fig. 1 where selected phenomena are characterized with very approximate spatial and temporal scales (defined here as the diameter and duration of the phenomena). For example, mesocyclones

Unauthenticated | Downloaded 02/01/24 06:03 PM UTC

are very approximately 3–10 km in diameter and persist for 1,000–3,000 s. It takes at least five observations across the diameter (or duration) of a phenomenon, each with a beamwidth (or sample time) 1/4 of this distance (or time), to well resolve its characteristics (measure about 90% of the magnitude) (Carbone et al. 1985). The 1/4-scale observations necessary for a mesocyclone to be well resolved range from 0.8 to 2.5 km, and from about 300 to 800 s. A WSR-88D observing severe weather conducts a volumetric update every 300 s, temporally well resolving most mesocyclones. However, the ability of WSR-88Ds to well resolve mesocyclones spatially depends on the range to the mesocyclones, and the resulting beamwidth of the observations. Very approximately, WSR-88Ds are spaced at 200-km intervals and have 200-km observational domains, so about 50% of mesocyclones occur within 141 km of WSR-88Ds. But the beamwidth at 141 km is about 2.5 km, which is barely able to well resolve detailed characteristics of large mesocyclones. So, while WSR-88D radars can *detect* mesocyclones through much of their observational domain, they can only *well resolve* large mesocyclones over about 1/2 of that area. Tornadoes, with diameters ranging typically from 100 to 800 m (Wurman et al. 2021) and lifetimes ranging typically from 100 to 1,200 s, require observational scales of 25–200 m and 25–300 s to be well resolved. This is only achieved when long-lived large tornadoes pass within 4 km of a WSR-88D, i.e., only very rarely. It is important to note that resolving the detailed characteristics of phenomena such as tornadoes, microbursts, and mesocyclones is critical for scientific studies, it is not necessary in order to inform severe weather warnings. WSR-88D data provide great benefit to the warning process through direct detection and indirect inference of the presence or likelihood of these phenomena.

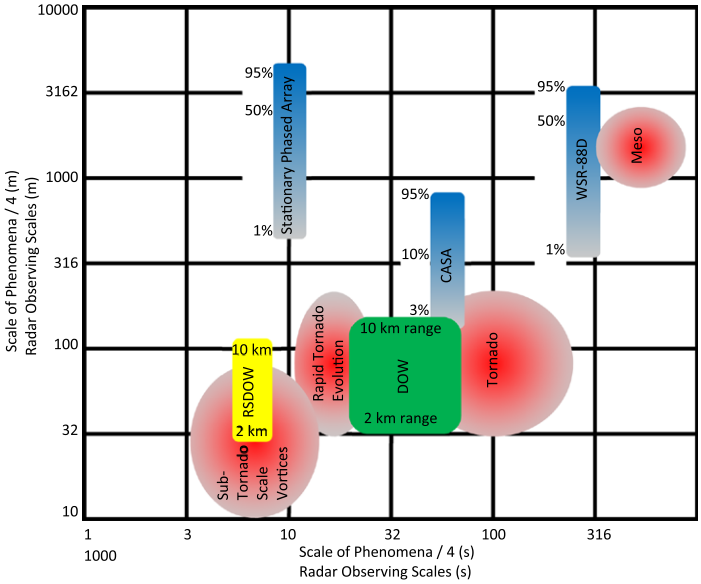

Fig. 1. What radars can and cannot resolve: 1/4 scales (diameters) of phenomena compared to radar observing scales (logarithmic axes) reveal whether radars can well resolve various phenomena. For example, to well resolve a 10-km diameter mesocyclone with an ~2,000-s temporal scale (duration), observations with scales of <2.5 km and <500 s are required. The fraction of the full observing domain achieving given spatial resolutions is illustrated for stationary radars. The spatial scale achieved by MQD DOWs are shown at 2- and 10-km deployment ranges to observed phenomena. The WSR-88D network can spatially well resolve large mesocyclones throughout about 1/2 of its observing domain. But they spatially well resolve tornadoes over ≪1% of their domain and cannot well resolve tornadoes temporally. Faster-scanning sparse phased array networks could well resolve tornadoes temporally, but not spatially. Denser arrays of fast-scanning stationary radars, e.g., CASA, would not spatially well resolve most tornadoes. MQD DOWs can well resolve many, but not all tornadoes spatially. Rapid-scanning MQD such as the RSDOW are required to well resolve rapid tornado evolution, sub-tornado-scale vortices, and other rapidly evolving atmospheric phenomena such as turbulent fire plumes, boundary layer eddies, and hurricane tornado-scale vortices.

Sparse rapid-scanning phased array networks could well resolve temporal but not spatial scales of tornadoes. Dense quick-scanning arrays such as Collaborative Adaptive Sensing of the Atmosphere (CASA; Junyent et al. 2010) can very well resolve mesocyclones and tornadoes temporally but cannot spatially well resolve most tornadoes.

Solution: Adaptable arrays of mobile/quickly deployable radars. The most effective solution to two of these limitations, spatial resolution and lower observing horizon, is also the simplest: *get closer.*

Unauthenticated | Downloaded 02/01/24 06:03 PM UTC

The most efficacious, moderate-cost, and widely employed solution, pioneered by the Doppler on Wheels (DOW) network, has been the deployment of single or multiple truck-mounted MQD pencil-beam-scanning radars (Wurman et al. 1997). DOWs, and other MQD radars [Bluestein and Pazmany 2000; Biggerstaff et al. 2005; Weiss et al. 2009; Pazmany et al. 2013; NSSL 2021; UAH 2021] have proven particularly valuable tools to observe rare, intermittent, localized, and quickly evolving and propagating phenomena, particularly in the common situation where the details of mesoscale phenomena evolution are not well forecast hours in advance. MQD radars target mesoscale phenomena when and where they occur, increasing the number of sampled phenomena and the quality of observations. MQD DOWs, described below, simply by getting closer and scanning more quickly, are able to resolve the spatiotemporal scales of many important mesoscale phenomena including microbursts, boundary layer thermals, hurricane boundary layer rolls, tornadoes, gust front structures, and lake-effect snowbands. The ability of DOWs to well resolve the spatial and temporal scales depends on the range to the phenomenon and the duration and evolutionary time scale of the phenomenon. Referring to Fig. 1, DOWs, at typical deployment range of 2–10 km, conducting quick volumetric scans at 20–80-s intervals, are able to well resolve the spatial and temporal scales of many, but not the smallest tornadoes. Resolving rapid changes in tornado structure, or sub-tornado-scale multiple vortices requires both very fine spatial-scale observations and rapid scanning, as provided by the Rapid-Scan DOW (RSDOW) ("Rapid-Scan DOW" section).

The DOWs have been deployed semipermanently (e.g., for weeks or months) in remote locations, anywhere there is even a four-wheel drive road. These missions include long-term deployments to remote/challenging areas [e.g., AgI Seeding Cloud Impact Investigation (ASCII; Geerts et al. 2013), Seeded and Natural Orographic Wintertime Clouds: The Idaho Experiment (SNOWIE; Tessendorf et al. 2019), Olympic Mountains Experiment (OLYMPEX; Houze et al. 2017), BRISTOL-HEAD]. Nomadic, chasing, or seminomadic missions include VORTEX (Rasmussen et al. 1994), VORTEX2 (Wurman et al. 2012), Radar Observations of Tornadoes And Thunderstorms Experiment (ROTATE; Wurman 2003, 2008), Tornado Winds from In situ and Radars at Low level (TWIRL; Kosiba and Wurman 2016a), hurricanes (Wurman and Winslow 1998; Kosiba et al. 2013; Kosiba and Wurman 2014; Wurman and Kosiba 2018), Remote Sensing of Electrification, Lightning, and Mesoscale/Microscale Processes with Adaptive Ground Observations (RELAMPAGO; Nesbitt et al. 2021), long-lake-axis parallel (LLAP; Steiger et al. 2013), OWLeS (Kristovich et al. 2017), Plains Elevated Convection At Night (PECAN; Geerts et al. 2017), Mesoscale Alpine Programme (MAP; Bousquet and Smull 2003), Juneau Airport Wind System (JAWS; Mueller et al. 2004), Intermountain Precipitation Experiment (IPEX; Schultz et al. 2002), and Convective and Orographically Induced Precipitation Study (COPS; Wulfmeyer et al. 2008). (See supplemental materials table for listing of research projects and project acronyms; https://doi.org/10.1175/BAMS-D-20-0285.2.)

Why mobile/quickly deployable targeted surface and sounding arrays?

Value and limitations of stationary ground-based observational arrays. In situ measurements of state variables (e.g., T, RH, P, winds) are critical for understanding meteorological phenomena. However, operational surface and upper-air sounding meteorological networks, including specialized regional surface networks such as the Oklahoma Mesonet (Brock et al. 1995) the West Texas Mesonet (Schroeder et al. 2005), and MESOWEST (Horel et al. 2002), are usually too coarsely distributed to resolve the small scales associated with high-impact atmospheric phenomena. Just as with radars, to well resolve spatial scales < 10 km, in situ observational spacing ≪ 10 km is required. Tiling a 300 km × 300 km study region at 1-km (or 5 km) spacing, only capable of well resolving phenomena with scales > 4 km (or >20 km) (see "Why mobile/quickly deployable targeted radar arrays?" section) would require 906,000 (301^2)

Unauthenticated | Downloaded 02/01/24 06:03 PM UTC

[or 3,700 (61^2)] instruments, likely an impractical endeavor (see also Trapp 2013, section 3.5). Even this ambitious stationary design would still be at substantial risk of missing desired events falling outside the study region. Slowly deployable research mesonets (e.g., Foote and Fankhauser 1973; Brock and Govind 1977) have had to choose between very small observational domains and very coarse spacing.

Solution: Arrays of "mobile," quickly deployable, ground-based instrumentation. The modern paradigm for obtaining critical in situ state variable observations in mesoscale studies utilizes adaptable observing systems, which can be easily and quickly deployed ahead of, or during, phenomena of interest. Broadly, these systems fall into three categories:

1) MQD mobile mesonets (MM), where instruments are mounted on vehicles that are driven to phenomena of interest and sample by driving through or near these phenomena (e.g., Straka et al. 1996),
2) QD instruments that are placed ahead of phenomena and remain stationary throughout the data collection {e.g., Totable Tornado Observatory (TOTO; Bedard and Ramzy 1983; Bluestein 1983), Turtles (Brock et al. 1987; Winn et al. 1999), StickNet (Schroeder and Weiss 2008), Florida Coastal Monitoring Program 10-m towers (Masters et al. 2010), deployable weather stations [Hardened In situ Tornado Pressure Recorder (HITPR; Lee et al. 2004; Wurman and Samaras 2004)], disdrometers (Friedrich et al. 2013), and Pods (Wurman et al. 2012)}, and
3) QD and MQD upper-air and boundary layer balloonborne sounding systems (e.g., Rust et al. 1990; Trapp et al. 2016; Markowski et al. 2018b).

Mobile Mesonet transects, QD surface instrumentation, and MQD soundings through features such as drylines, fronts, storm-generated boundaries and cold pools yield cross-frontal/boundary data, which allow for mapping and characterizing moisture, wind, and temperature variations that can influence storm initiation, development, and evolution. Targeted in situ observations using the FARM systems described below, often augmenting DOW or other MQD radar observations, have been, or can be used to increase understanding of a myriad of phenomena including snowbands (Kosiba et al. 2020), urban impacts, wind farm effects, storm anvil and fire plume shadow effects, terrain effects, deep convection (Trapp et al. 2020; Schumacher et al. 2021; Nesbitt et al. 2021), cold pools (Kosiba et al. 2018b), hurricanes (Kosiba and Wurman 2009; Kosiba et al. 2013; Wurman et al. 2013b; Wurman and Kosiba 2018a; Kosiba and Wurman 2018), and tornadic storms (Markowski et al. 2002; Wurman et al. 2007a; Markowski et al. 2012a; Kosiba et al. 2013b; Kosiba and Wurman 2013; Wurman et al. 2013a). (See supplemental materials table.)

Invention, development, deployments of the DOWs and other systems

Targeted single-DOW observations: DOW1 and successors. While QD, even truck-mounted, nonmeteorological radars had existed for decades (Fink 1945), and continuous-wave (e.g., Bluestein and Unruh 1989) and special purpose millimeter-wave (e.g., Bluestein et al. 1995) systems had been used in limited applications for research, the DOW radars (Wurman et al. 1997) were the first general-purpose MQD weather radars capable of quick scanning volumetric data collection, very fine-scale resolution with pulsed transmissions and narrow "pencil beams," and abilities to penetrate a wide variety of meteorological phenomena using centimeter-wavelength transmissions.

The first DOW prototype was constructed during October 1994–May 1995, for <$50,000, using surplused parts from the National Center for Atmospheric Research (e.g., the old CP-2 radar transmitter; Keeler et al. 1989), a repurposed Econoline Van provided by the National

Unauthenticated | Downloaded 02/01/24 06:03 PM UTC

Severe Storms Laboratory, and a surplus SCR-584 antenna (Fink 1945). Signal processing and antenna control were hosted on now considered primitive 486 and 286 computers, with data stored on Exabyte tapes. The DOW (later named DOW1) (Fig. 2) deployed during the final weeks of the VORTEX tornado study. New DOW data immediately heralded a qualitative improvement in the ability to observe the fine-scale structure and evolution of tornadoes (e.g., Wurman et al. 1996; Wurman and Gill 2000; Wurman and Kosiba 2013) and a paradigm change for many mesoscale observational studies. The DOW prototype was in a nearly continuous state of evolution as the frontiers of this new technology and its applications were expanded. From 1995 to 1997, the 1.83-m-diameter antenna was replaced with a 2.44-m unit, reducing beamwidth from 1.22° to 0.93°. New, faster, and more powerful antenna motors permitted high-speed scanning > 50° s^{-1}, even in strong winds, and while driving. A more powerful transmitter and improved signal processing systems and computers were installed. Data were recorded to compact disks (2020-era DOWs would fill one of these compact disks every ~10 s). Faster leveling systems allowed precisely navigated data to be collected <50 s after parking. Basic specifications of DOW1 and other FARM radars are found in Table 1. The FARM website (http://farm.atmos.illinois.edu) has links to loops, project descriptions, additional imagery and documentation, data servers, and articles/books describing facility components.

Fig. 2. DOW1 MQD radar in 1995 (from Wurman et al. 1997).

The new observing paradigm of deploying a high-capability radar near tornadoes enabled the harvesting of many and varied scientific "low-hanging fruit" by DOW1 and its successor DOWs (described below). These include the first tornado wind maps, measurements of an axial downdraft and lofted debris (Wurman et al. 1996; Wurman and Gill 2000), multiple vortices (Wurman 2002; Alexander and Wurman 2005), winds versus damage and surface measurement intercomparisons (Wurman and Samaras 2004; Wurman and Alexander 2005; Kosiba and Wurman 2013; Wurman et al. 2013a) (Fig. 4e), winds as low as 3–4 m AGL and low-level inflow (Wurman et al. 2007c; Kosiba and Wurman 2013), 3D ground-based velocity track display (GBVTD) vector wind field retrievals (Lee and Wurman 2005; Kosiba and Wurman

Table 1. FARM radar specifications.

Basic specs	DOW1	DOW2,3	DOW 6,7	COW	DOW 8	RSDOW
Tx (kW peak)	40	250	2 × 250	2 × 1,000	100	40
PRF (Hz)	500–2,000 (later 500–4,000) w/stagger	500–5,000 w/stagger	500–6,000 w/stagger			
Pulse length (μs)	0.5–1.0 (later 0.25–1)	0.167–1.0	0.167–1.0			0.1–1.0
Scan rate (° s^{-1})	30 (later 50)	50	50	24	50	7-s vols
Products	*Z*, *V*, NCP, SW	*Z*, *V*, NCP, SW	LDR, Z_{DR}, ρ_{HV}, *V*, *Z*, SW, NCP, IQ		*Z*, *V*, SW, NCP, IQ	
Beamwidth (°)	1.22 (later 0.93)	0.93	0.93	1.05	0.93	0.8 × 0.9
Gate length (m)	75–300 (later 25–300)	12.5–600	12.5–600			11–600
Meteorological and comm mast	None	10 m	18 m	Future mast	14 m	

Unauthenticated | Downloaded 02/01/24 06:03 PM UTC

2010), rapid evolution of debris over varying land use and terrain (Burgess et al. 2002; Kosiba et al. 2012), documentation of cyclonic/anticyclonic tornado pairs and documentation of varied and complex tornado wind field structures including multiple wind field maxima and multiple vortex mesocyclones (Wurman and Kosiba 2013), downward propagation of vorticity (Wurman and Alexander 2005) and an extensive climatology of tornado intensity and size revealing, quantitatively, that tornadoes are much more intense and larger than indicated by damage surveys (Wurman et al. 2021). The DOWs have documented the largest and most intense tornado wind fields ever measured (Wurman 2003; Wurman et al. 2007c, 2014), and even, unintentionally, collected data from inside some tornadoes. DOW data were first used to constrain and compare to large-eddy simulations of tornado vortices (Kosiba 2009) and laboratory models (Refan et al. 2014), and provide a comparison of tornadic intensity to WSR-88D observations (Toth et al. 2013). DOW data have been integrated with photogrammetric analyses of tornadoes (Wakimoto et al. 2011, 2012). (Multiple-DOW deployments and vector wind studies are discussed in the next section.)

The DOW1 was deployed into Hurricane Fran (1996), pioneering land-based scientific hurricane intercepts and discovering an unexpected phenomenon, quasi-linear hurricane boundary layer rolls (HBLR) (Wurman and Winslow 1998), found to be ubiquitous (e.g., Morrison et al. 2005; Lorsolo et al. 2008; Kosiba et al. 2013) (Fig. 4b). A DOW mission in Hurricane Harvey (2017) revealed the existence of intense tornado-scale vortices (TSV) linked to swaths of wind damage and mapped eyewall mesovortices (Wurman and Kosiba 2018a) (Fig. 4c). TSVs also were observed in Hurricane Irma (2017) (Kosiba and Wurman 2018). The DOWs documented that tall buildings could cause narrow regions of reduced hurricane winds several km downstream (Wurman and Robinson 2013).

It was realized very quickly that DOWs could be utilized in a wide variety of observational programs beyond tornadoes and hurricanes. Immediately after VORTEX, DOW1 was deployed to observe convective initiation and boundary layer rolls in Small Cumulus Microphysical Study (SCMS) and Flatland/Lidars In Flat Terrain (LIFT; Weckwerth et al. 1999) and for an MIT microburst study in New Mexico in 1996. Between 1995 and 2020, DOW1 and its successors were deployed to study many different phenomena throughout the United States, including Alaska and Hawaii, to Canada, Europe, and South America (Fig. 3 and supplemental material table). Selected scientific highlights include the following: DOWs were first to provide radar evidence of precipitation directly caused by cloud seeding (Tessendorf et al. 2019) (Fig. 4h), the first to map snowband misovortices (Steiger et al. 2013) (Fig. 4d), and first to produce fine-scale radar mapping of fire plumes and hot spots (Wurman and Weygandt 2003). The DOWs mapped fire retardant plumes, simulated aircraft-released toxin plumes, mapped dust devil winds (Wurman et al. 1997), examined coastal low-level jets and their impact on heavy rainfall (Ralph et al. 1999), mapped the flow in alpine valleys (Bousquet and Smull 2003), examined descending reflectivity cores (DRC) in supercells (Byko et al. 2009), documented low reflectivity regions (LRR) in supercells (Wurman et al. 2012; Kosiba et al. 2013b), and mapped boundary layer stratification in nor'easters (NSF 2015) (Fig. 4g). DOWs have been used extensively to support education ("Education and outreach" section).

Targeted multiple-DOW network. The atmospheric equations of motion describe the evolution of 3D vector wind fields, not radar-measured Doppler "velocities." Updrafts, downdrafts, rotation, development of clouds and precipitation and lightning are all driven at least in part by 3D vector winds. *It is a rare consumer of Doppler velocity data who would not prefer access to vector wind field measurements*. Techniques for obtaining vector wind fields from multiple radar measurements are well established (e.g., Armijo 1969; Ray et al. 1975; Gao et al. 1999;

Unauthenticated | Downloaded 02/01/24 06:03 PM UTC

Fig. 3. Sample DOW deployments. (a) Schematic map of study domains, (b) DOW largely buried in snow at Snowbank, Idaho (2017), (c) DOW observing boundary layer during eclipse (2017), (d) DOW on Cape Cod during nor'easter (2015), (e) DOW during Hurricane Delta (2020), (f) DOW7 cabin interior, (g) DOW observing CalWood fire (2020), (h) flooded DOW site in Lake Quinault during OLYMPEX (2016), and (i) DOW scanning a tornado (2005).

Shapiro et al. 2009), as are more restricted techniques for inferring 3D winds from single-radar data (e.g., Browning and Wexler 1968; Lee et al. 1994).

To obtain fine-scale multiple-Doppler vector wind measurements, all of the individual radars must be close to the targeted phenomena (see Fig. 1 in Wurman et al. 1997), which is

Unauthenticated | Downloaded 02/01/24 06:03 PM UTC

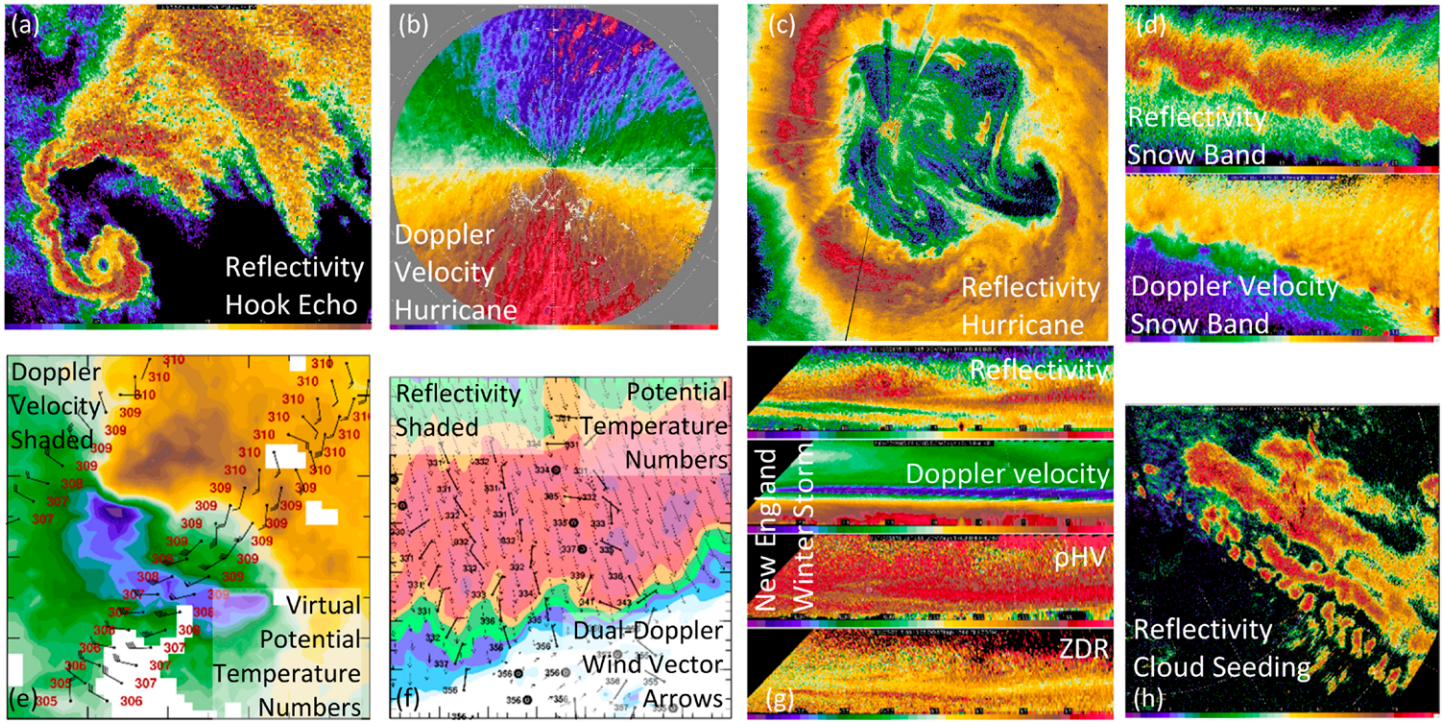

Fig. 4. Illustrative FARM data images. (a) Tornadic hook echo, (b) hurricane boundary layer rolls, (c) interior view of hurricane eye with mesovortices, (d) lake-effect snowband misovortices, (e) integrated radar and in situ observations of a tornado, (f) integrated radar and in situ observations in a mesoscale convective system, (g) vertical (RHI) slice of microphysical layering during nor'easter, and (h) snowbands/cells caused by cloud seeding.

difficult to achieve with stationary radar networks. This, and the simple benefit of increasing single-DOW observational coverage, motivated the creation of the multiple-DOW network, with the construction of DOW2, in 1997, and its successors.

As was the case with single-DOW deployments, many targeted multiple-DOW deployments harvested "low-hanging scientific fruit." Multiple-DOW tornado "chasing" missions allowed creation of the first fine-scale vector wind field maps of tornadic storms, revealing secondary rear flank gust fronts, fields of vorticity, divergence, tilting of vorticity near tornadoes, and triggers for tornadogenesis (e.g., Wurman et al. 2007a,b; Marquis et al. 2008; Wurman et al. 2010; Marquis et al. 2012; Markowski et al. 2012a,b; Kosiba et al. 2013b; Markowski et al. 2018a), and the first dual-Doppler vector winds resolving tornado structure (with RaXPoL) (Wurman et al. 2016).

Quick, as well as semipermanent deployments were used to create vector wind mapping of a wide range of other phenomena including nontornadic supercells (e.g., Beck et al. 2006; Frame et al. 2009), convection initiation and the role of misocyclones (Arnott et al. 2006; Marquis et al. 2007; Ziegler et al. 2007; Friedrich et al. 2008), lake-effect snowbands and embedded misocyclones (Mulholland et al. 2017; Kosiba et al. 2020), nocturnal mesoscale convective systems (Kosiba et al. 2016b; Miller et al. 2020), deep convective storms in complex terrain (Weckwerth et al. 2014; Trapp et al. 2020), and agricultural effects on the boundary layer (Rappin et al. 2021). Fluxes and turbulent kinetic energy (TKE) associated with sub-kilometer-scale hurricane boundary layer rolls were quantified (Kosiba and Wurman 2014). The first vector wind retrievals of the boundary layer in a total solar eclipse (Wurman and Kosiba 2018b) and in and near wildfire plumes were obtained by DOWs in 2017 and 2020, respectively. Multiple DOWs were used for marine boundary layer studies during CMRP, and for educational missions during Pennsylvania Area Mobile Radar Experiment (PAMREX) (Richardson et al. 2008). DOW vector wind fields have been integrated with photogrammetric analysis (Atkins et al. 2012) (see supplemental materials table).

Unauthenticated | Downloaded 02/01/24 06:03 PM UTC

Rapid-Scan DOW. DOW sampling volumes can be 20,000 times smaller than that typical of WSR-88Ds. For example, at typical ranges between targets and these radars:

- WSR-88D resolution volume at 100-km range: 1,667 m × 1,667 m × 250 m = 7×10^8 m^3
- DOW resolution volume at 2-km range: 33m × 33m × 25 m = 3×10^4 m^3

However, typical DOW *temporal* resolution is only several times better than that of WSR-88D's, 300-s volumes versus 60 s. The DOW-obtained ultrasharp "snapshots" of tornadoes revealed that substantial evolution sometimes occurred between observations (Wurman et al. 2007a), limiting the understanding of these evolutionary processes. This effect is clear in Fig. 1, showing how proximate DOWs can well resolve the spatial scales of tornadoes, but not rapid changes. The need for more rapidly scanning radars has long been known (e.g., Keeler and Frush 1983). But rapid scanning alone, e.g., a network of phased array systems spaced similarly to the current WSR-88D network, results in more frequent but very blurry data (Fig. 1), unable to resolve small spatial scales. *Balanced fine spatial- and temporal-scale observations are required to fully resolve small and rapidly evolving systems such as tornadoes, microbursts, misocyclones, hurricane boundary layer rolls, boundary layer thermals, rapid fire plume evolution, and the like*, motivating the development of the Rapid-Scan DOW (RSDOW) (Wurman and Randall 2001), which became operational in 2003 (Fig. 5).

The RSDOW employs a relatively inexpensive and "low tech" slotted waveguide antenna. Multiple frequencies are transmitted quasi simultaneously from a traveling wave tube (TWT) transmitter, in a "frequency-stepped chirp" pulse (see Wurman and Randall 2001), emitting several wavelengths quasi simultaneously. Unlike slotted waveguide array antennas used in other multifrequency radars such as ELDORA (Hildebrand et al. 1996), the RSDOW antenna is purposely very dispersive, steering these emissions at different frequencies in different directions, resulting in multiple quasi-simultaneous beams pointing at different elevations (see Fig. 5). The sky is "raked" at several different elevation angles nearly simultaneously. Data from each frequency, and therefore each differently pointing beam, are processed separately, as if it were from a different radar, resulting in volumetric data as fast as the antenna completes 360° rotations, typically every 7 s. As with all FARM radars, RSDOW archives all raw time series ("IQ," the in-phase and quadrature components of the complex raw signal; see Doviak and Zrnić 1984) data, permitting custom and experimental postprocessing, resampling, and filtering. Frequency dithering (changing frequency by a few tens of megahertz every 1/2° of azimuthal scanning, to change beam elevation pointing by about 1/2°) to improve

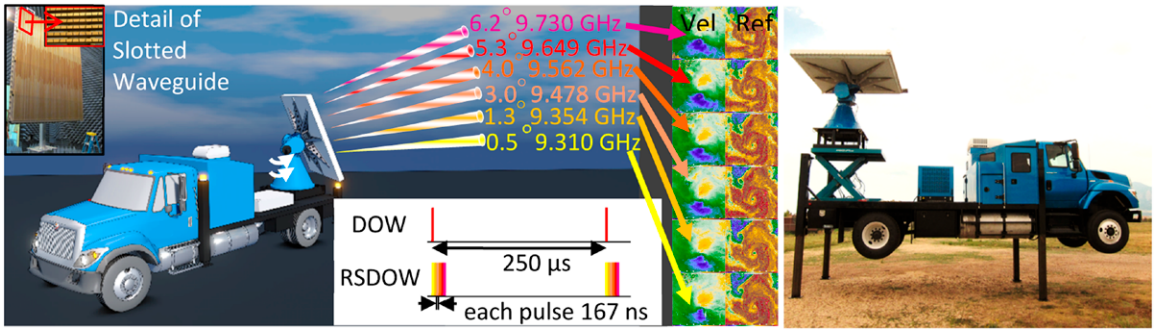

Fig. 5. (left) Rapid-scan DOW (RSDOW) slotted waveguide antenna transmits several simultaneous beams at different elevations using stepped-chirp pulses. Simplified DOW and RSDOW pulse sequences are compared schematically. Mechanical azimuthal scanning rakes the sky at all the elevations, resulting in volumetric data every 7 s. (center) Simultaneous Doppler velocity and reflectivity slices from different elevations in a tornado. (right) RSDOW with legs and scissor lift extended.

Unauthenticated | Downloaded 02/01/24 06:03 PM UTC

vertical resolution, and other specialized transmit/receive techniques are possible with the RSDOW, but have not been used to date.

The RSDOW data revealed short-period wind speed oscillations in a tornado (Wurman et al. 2013a) attributed to small spatially unresolved multiple vortices and documented for the first time that the most intense winds in a different tornado were below 10 m AGL (Kosiba and Wurman 2013). The RSDOW collected fine-temporal-resolution data in snowbands during OWLeS, in a variety of supercellular thunderstorms during VORTEX2, measured the rapid evolution of hurricane boundary layer rolls during Hurricanes Isabel (2003) (Wurman 2004) and Isaac (2012) (Wurman et al. 2013b) and deployed for the University of Colorado Boulder Teaching flow Over Mountains (CU-TOM) and Texas A&M University Student Operational Aggie Doppler Radar Project (TAMU-SOAP) educational projects (see supplemental materials table).

The RSDOW platform can be converted to host a traditional radar, for projects which do not require extremely rapid volumetric updates. A 250-kW transmitter, 0.9° beam parabolic antenna, and different receiver and signal processing replace the specialized RSDOW components, and the system is fielded as DOW8. The RSDOW/DOW8 platform hosts a 14-m pneumatic mast on which anemometers and VHF radio antennas are usually mounted. Temperature (T), relative humidity (RH), and pressure (P) instrumentation are mounted to the truck. A scissor lift can raise the pedestal about 2 m so that the antenna is above the height of the operator and driver cabin, but this has not, to date, been used during a mission.

Quick-scanning dual-polarization DOWs. Dual-polarization radars (Bringi and Chandrasekar 2001; Fabry 2015; Rauber and Nesbitt 2018; Bringi and Zrnić 2019) have been used in meteorological research dating back to the 1980s (e.g., Wakimoto and Bringi 1988) to provide observations distinguishing hail, drop size, and other precipitation particle characteristics. Recognizing the added information provided by dual-polarization capabilities, the WSR-88D network was upgraded to dual polarization from 2011 to 2013. The University of Massachusetts MQD radar was upgraded to dual polarization, obtaining pioneering observations of tornado debris clouds (Bluestein et al. 2007). The NOAA NOXP became operational prior to deploying in Hurricane Ike in 2008 (NSSL 2021). The University of Alabama upgraded the Advanced Radar for Meteorological and Operational Research (ARMOR) radar in 2004 (Petersen et al. 2004).

A critical limitation of dual-polarization systems was that they must scan slowly to obtain the necessary independent samples required for accurate dual-polarization measurements (Bringi and Chandrasekar 2001). Slow scanning is an anathema for targeted short-temporal-scale studies of rapidly evolving phenomena (see Fig. 1). So, to permit more balanced temporal- and spatial-scale dual-polarization observations, two DOWs (DOW6 and DOW7) were upgraded to dual polarization, employing a unique dual-polarization, dual-frequency (DPDF) design. The DPDF technique involves transmitting two frequencies quasi simultaneously, separated by 150 MHz. This permits independent samples from each frequency to be combined, allowing for high quality Z_{DR} calculations while scanning twice as fast. The DPDF DOWs employ a unique polarization switching array (Fig. 6) permitting two different transmit/receive modes:

- "Fast-45": Both frequencies transmit at 45° polarization orientation (by transmitting equal power at both horizontal and vertical polarizations simultaneously) and measure returned horizontal and vertical signals in order to calculate differential reflectivity (Z_{DR}), cross-polarization correlation coefficient (ρ_{HV}), and differential phase (Φ_{DP}) in both frequencies.
- "LDR+45": One frequency is emitted with a horizontal polarization angle, permitting calculation of linear depolarization ratio (LDR) through comparison of horizontal and vertical polarization returns. The second frequency is transmitted at 45° orientation, as

Unauthenticated | Downloaded 02/01/24 06:03 PM UTC

described above, allowing calculation of Z_{DR}, ρ_{HV}, and Φ_{DP}. LDR+45 mode was first used during RELAMPAGO (Trapp et al. 2020).

The DPDF DOWs archive all raw time series ("IQ") data, permitting custom and experimental postprocessing, resampling, and filtering. DPDF DOWs were used in VORTEX2, LLAP,

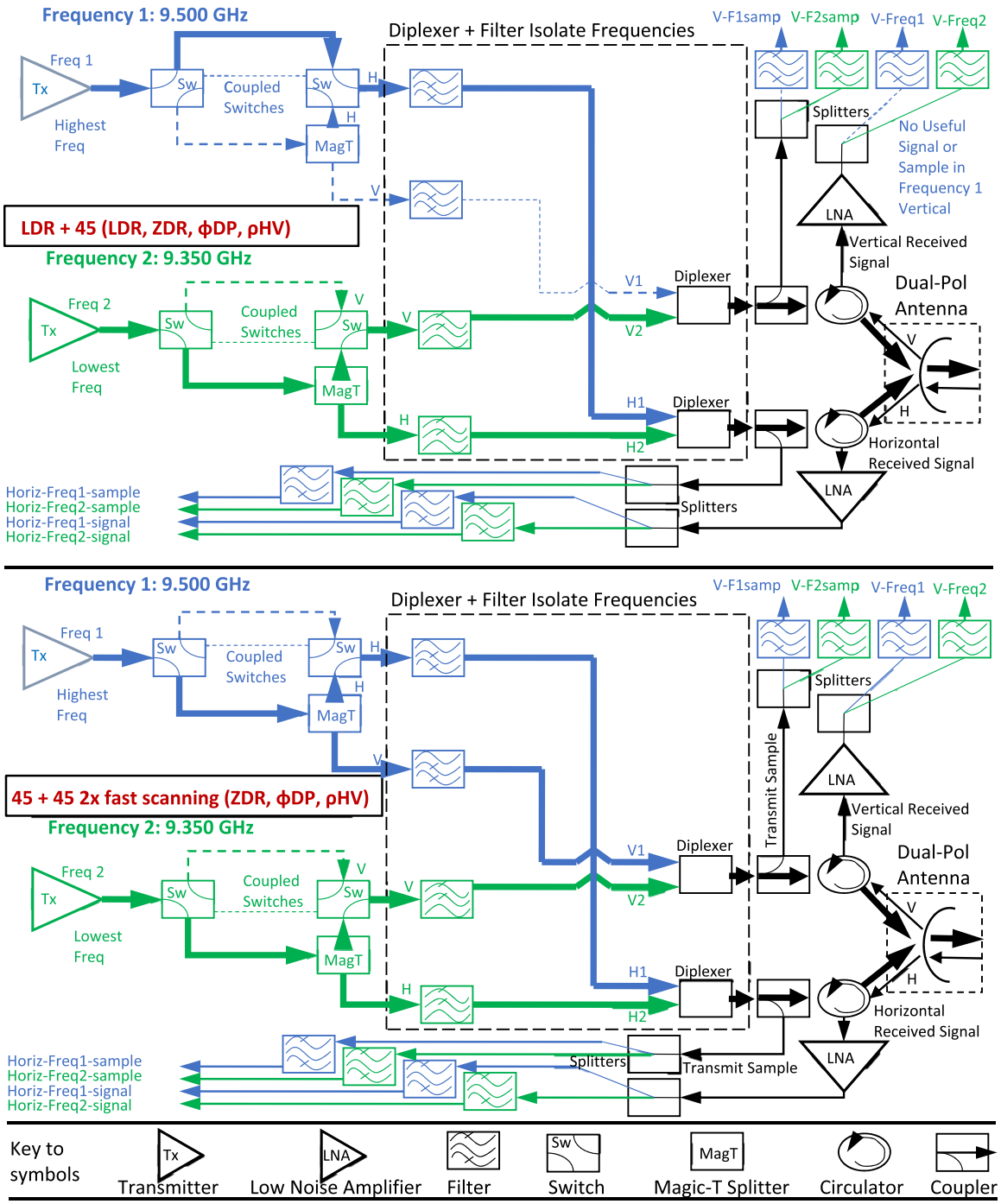

Fig. 6. Simplified block diagram of dual-frequency dual-polarization (DPDF) DOW design. (top) In LDR+45 mode, frequency 1 (blue paths) is transmitted at horizontal polarization and frequency 2 (green paths) at 45°, permitting LDR calculation. Both frequencies are combined in diplexers, then transmitted and received quasi simultaneously (black paths). (bottom) Flipping coupled switches enables Fast-45 mode, in which both frequencies are transmitted at 45°, resulting in doubled independent samples, permitting twice-as-fast dual-polarization scanning. Heavy lines indicate "hot" transmission paths. Horizontal and vertical polarization received signals and transmit pulse samples are sent to receivers and signal processors.

Unauthenticated | Downloaded 02/01/24 06:03 PM UTC

TWIRL, Great Plains Irrigation Experiment (GRAINEX), SNOWIE, ASCII, OWLeS, PECAN, and RELAMPAGO (see supplemental materials table). The DPDF DOW platforms host 18-m pneumatic masts on which anemometers and VHF radio antennas are usually mounted. The *T*, RH, *P* instruments are mounted to the trucks.

C band on Wheels. The FARM (and all other MQD) radars employ antennas smaller than 2.5 m so that the trucks plus antennas can fit on roads and under bridges. To focus narrow, ≤1° beams, most MQD radars transmit using wavelengths from 3 mm (W-band) to 3 cm (X-band). The paramount goal of fine-scale resolution is achieved, but at the cost of severe attenuation in heavy precipitation, common in high-impact mesoscale systems. A notable exception has been the C-band (~5.5 GHz or 5 cm) Shared Mobile Atmospheric Research and Teaching (SMART) radars (SRs) (Biggerstaff et al. 2005), which suffer less attenuation (Fig. 7) (see, e.g., Doviak and Zrnić 1984). But this ability comes with a cost. The SR's 2.4-m antennas produce broader beamwidths (1.6°) and >2.5 times larger resolution volumes (1.6°/0.93° horizontal × 1.6°/0.93° vertical) compared to X-band MQD radars such as the DOWs. The compromises inherent with X- and C-band mobile radars were experienced during VORTEX2 when SR2 and DOW6 simultaneously observed a tornadic supercell from similar ranges. The DOW6 observations were severely attenuated through the core, particularly behind the hook echo. SR2 observations severely underresolved the tornadic circulation, with observed shear of only 57 m s^{-1} compared to the DOWs measurement of 84 m s^{-1}, a reduction of 32% (Fig. 7).

To avoid the compromises inherent to existing X- and C-band MQD radars, the C band on Wheels (COW) was developed in 2018, using a unique quickly assembling

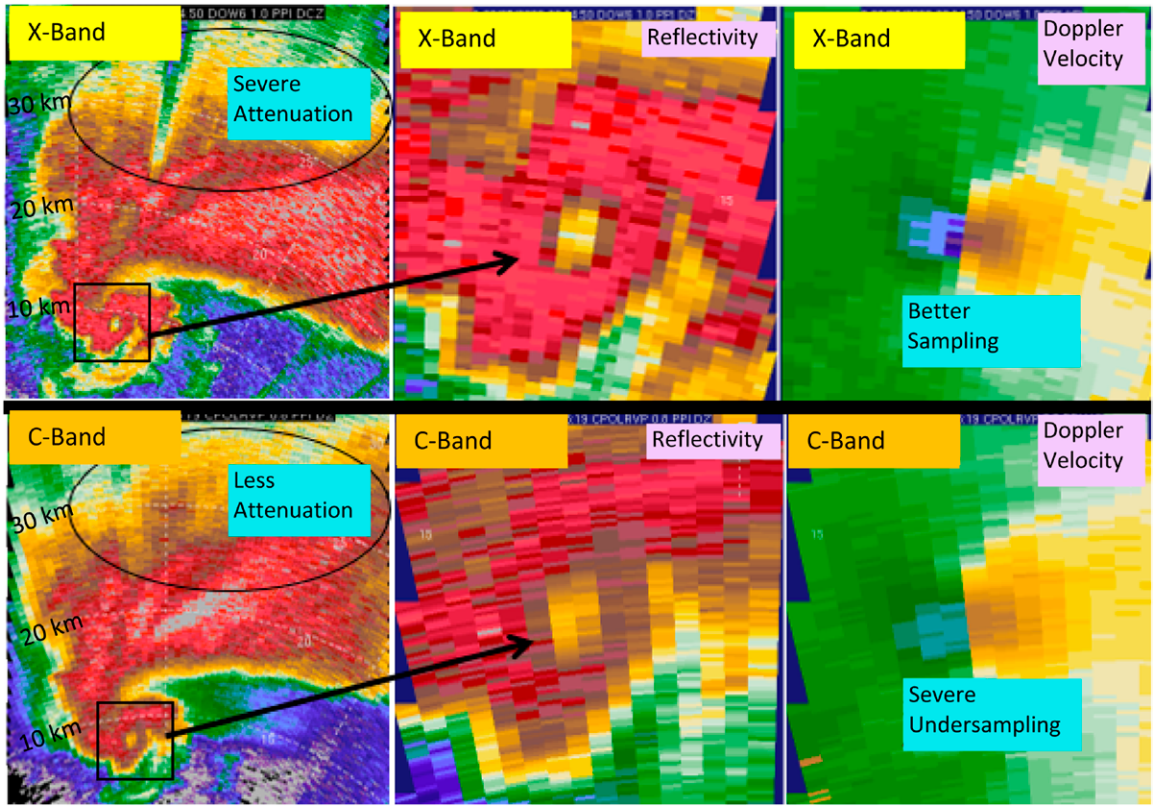

Fig. 7. C-band vs X-band attenuation, existing MQD radars. Comparison of SR C-band (1.6° beamwidth) and DOW X-band (0.93° beamwidth) observations of a supercell and tornado at about 10 km range to each radar, showing compromises between severe attenuation at X band and coarse resolution at C band. Scans are at approximately 1° elevation.

Unauthenticated | Downloaded 02/01/24 06:03 PM UTC

antenna design. The COW travels with its antenna in two pieces (Fig. 8). Then, using an onboard crane, this antenna is quickly assembled on-site, to its full 3.8 m diameter, resulting in a 1.05° beam. *Low attenuation and fine-scale resolution are achieved simultaneously.* Naturally, there is a compromise: the COW cannot "chase" since it requires ~2 h for setup and teardown. But the COW is ideal for most targeted observational projects, including those similar to RELAMPAGO, PECAN, Propagation, Evolution and Rotation in Linear Storms (PERiLS), IHOP, California Land-falling Jets Experiment (CALJET), and hurricanes, deploying up to once per day. And it can be deployed for longer periods for projects similar to OLYMPEX, GRAINEX, SNOWIE, and ASCII, and can also serve as a "gap filler" radar. Like the DOWs, the COW employs DPDF technology for Fast-45 dual-polarization and LDR+45 capability. COW uses dual 1-MW transmitters, by far the most powerful in any QD or MQD radar, for maximum sensitivity.

Fig. 8. COW assembly. COW as transported, antenna being assembled, antenna lifted onto pedestal, deployed.

MM, pods, poles, soundings, MORC

To provide a robust, integrated, and flexible in situ observational network deployable in coordination with the DOW/COW network, and to improve on existing designs for such observational systems, FARM includes an innovative, evolving and diverse array of MM and QD observational ground-based systems (PODNET, POLENET), several mobile upper-air sounding systems, a Lagrangian "swarmsonde" balloon system, and a Mobile Operations and Repair Center (MORC). Specifications are found in Table 2.

1) MM: Pickup-truck based MM with instruments that collect standard meteorological observations of *T*, RH, *P*, and wind incorporating pioneering forward-mounted 3.5 m AGL masts to avoid vehicle slipstream (Fig. 9). MMs carry PODNET units (see deployment of Pods from a MM in Fig. 10), balloonborne sounding systems, and disdrometers and can tow systems such as 915-MHz profilers.
2) PODNET: A pioneering array of QD ruggedized weather stations (Pods). Deployed from MM, Pods collect standard meteorological observations of *T*, RH, *P*, and wind at 1, 1.5, or 2 m AGL (depending on configuration), and video or time lapse photographs (Fig. 10).
3) Disdrometers: The facility hosts several Parsivel systems, which can be paired with dual-polarization radars and are often deployed with PODNET units.
4) POLENET: Often there is a need to obtain near-surface wind and other meteorological observations where there may be no solid and level ground, road shoulder, and/or at altitudes above 2 m AGL (in less open terrain, near fences, guard rails, road signs, or at flood-prone sites, etc., e.g., in a hurricane). The FARM includes an array of QD, fully

Unauthenticated | Downloaded 02/01/24 06:03 PM UTC

configurable, rugged instruments comprising POLENET. These are attached with clamps and/or straps to existing infrastructure such as telephone and power poles, bridge railings, dock railings, lighting poles, and similar structures (Fig. 11), in order to measure wind, *T*, *P*, and RH.

5) Soundings: Several GRAW and one Windsonde/Swarmsonde balloonborne sounding systems are operated from MMs, DOWs, or other vehicles to provide adaptable/targeted upper-air and boundary layer sounding capability (Fig. 12).
6) MORC: Complex highly mobile (chasing) projects such as VORTEX2, ROTATE, and TWIRL, or projects with special needs [e.g., Multi-Angle Snowflake Camera and Radar (MASCRAD)] may require a mobile operations/coordination center, data management office, and repair facility, or a field headquarters vehicle. The MORC is a long sprinter van with multiple scientist/engineer work stations, a wall of monitors, a computer rack, and two generators. A 10-m pneumatic mast houses weather instruments and a high-powered VHF radio for communications with mobile or remote fleets (Fig. 13).

The FARM MMs, with evolving designs, were used to obtain transects in and near supercellular thunderstorms and tornadoes (ROTATE, VORTEX2, TWIRL) (Fig. 4e), and even obtained, accidentally, observations from inside a tornado (Kosiba and Wurman 2013). PODNET was initially designed to obtain multiple transects of low-level tornado winds. The very simple and inexpensive and robust design allowed for many PODNET units to be constructed, and "picket fence" type deployments ahead of tornadoes to be attempted. Pods obtained wind data very near tornadoes (Kosiba et al. 2016a; Wurman et al. 2016; Kosiba et al. 2020b), revealing high potential temperature inflow toward tornadoes and possible inflow jets. Efforts continue to achieve the full picket fence style of deployment. PODNET was deployed on sea walls during Hurricane

Table 2. FARM in situ instrument specifications.

	PODNET	POLENET	Mobile Mesonet	Upper-air soundings	Disdrometers
Number	Up to 20	3–12 (can share instrumentation package with PODNET)	3	6 Graw 1 Windsond/ Swarmsonde	4
Measurements	*T*/RH (Campbell Scientific EE181-L/ Rotronic HC2S3 + Shield RAD10E) *P* (Vaisala PTB1100) GPS (Garmin 16X-HVS) Wind × 2 (RM Young Jr. 04101 and Gill WindSonic 75 Ultrasonic)	Wind (RM Young 05103 and FT742 sonic anemometers), can be customized with any PODNET instrumentation	*T*/RH (Campbell Scientific EE181-L + Shield) *P* (Vaisala PTB1100) GPS (Garmin 16X-HVS) Wind (RM Young 05103); can host others	*T*, RH, wind, *P*	Drop size distribution
Sampling rate	Up to 10 Hz	Up to 10 Hz	Up to 10 Hz	1 s	10 s
Real-time data	Yes	Yes	Yes	Yes	No
Platform	Hardened steel "T" stand	Attaches to infrastructure such as power and light poles, railings, at user specified heights	Pickup truck; can deploy PODNET and POLENET (also sounding systems; not proposed)	Graw WindSonic	OTT Parsivel
Height	Configurable (currently 1, 1.5, 2 m)	Configurable, on existing infrastructure Typically 3–10 m	3.5 m	1–20,000 m	1 m
Camera/video attachment	Yes	Yes	Yes	No	Yes
Comm compatibility	Cellular internet	Cellular internet	Cellular internet		
Data	Local	Local or wireless	Local or internet	Local	Local

Unauthenticated | Downloaded 02/01/24 06:03 PM UTC

Ike, where it was too hazardous for manned-instruments (Kosiba and Wurman 2009), and during Hurricanes Gustav, Isaac, Harvey, and Irma (Wurman et al. 2013b; Wurman and Kosiba 2018a; Kosiba and Wurman 2018). Prototyping of POLENET occurred during Hurricane Florence (2018) and it deployed to collect ~4 m AGL winds in the landfall region of Hurricane Delta (2020)(Fig. 11).

The MMs and Pods documented thermodynamic variations across lake-effect snowbands during OWLeS (Kosiba et al. 2020), thunderstorm-generated cold pools during PECAN (Kosiba and Wurman 2016b) (Fig. 4f) and RELAMPAGO (Trapp et al. 2020; Nesbitt et al. 2021), and in New England coastal storms (NSF 2015). The FARM MQD upper-air sounding systems have been used in several studies including PECAN, MASCRAD, GRAINEX, and RELAMPAGO and the Swarmsonde system was first used in severe convection in 2020. The facility's disdrometers were used in PECAN and RELAMPAGO.

Education and outreach

The simplicity, transportability, and adaptability of the DOW radars has facilitated their broad use in education and outreach (Fig. 14). Often MM, Pods, and/or soundings are used

Fig. 9. FARM mobile mesonets (MM).

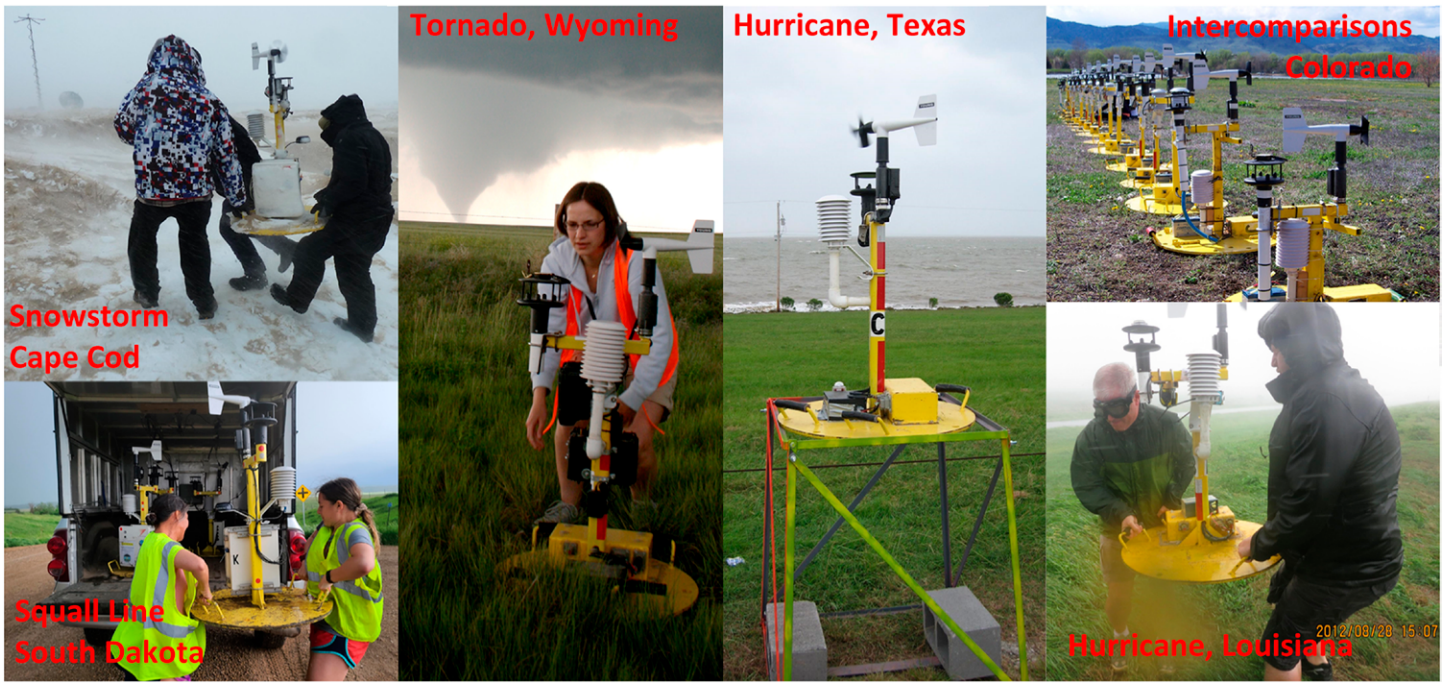

Fig. 10. FARM PODNET units.

Unauthenticated | Downloaded 02/01/24 06:03 PM UTC

in tandem with a DOW to provide a broader educational experience. *FARM is designed to be a national educational resource*. The DOWs, and other instrumentation, have participated in over 40 education and outreach projects at a variety of colleges and universities nationwide, most without major instrumentation programs themselves. These include small institutions, historically black colleges and universities (HBCU), and tribal colleges and universities (TCU), resulting in unusual and especially rich, hands-on exposure to otherwise unavailable state-of-the-art instrumentation. The DOWs have been integrated into radar, other meteorology, and environmental science courses (e.g., Richardson et al. 2008; Bell et al. 2015; Milrad and Herbster 2017) and have been used to facilitate local community and K–12 outreach. With only minor training, students can fully operate DOWs, resulting in hands-on, fully participatory educational experiences in experimental design, field data collection, and data analysis. Some student-designed projects have led to formal publications (e.g., Toth et al. 2011). The DOWs and associated instrumentation have been the highlight of small, large, and very large outreach activities both locally and nationwide, including a 20-museum national tour associated with an IMAX movie featuring DOW science missions, national events such as the U.S. Science and Engineering festival, and multischool tours such as occurred in Missouri in 2012. FARM instrumentation, data, and/or scientists have been featured in two IMAX films, *Forces of Nature* and *Tornado Alley* (Casey 2011), several documentaries including National Geographic's *The True Face of Hurricanes* and *Tornado Intercept*, Public Broadcasting's *NOVA*, and the Discovery Channel's *Storm Chasers* television series, as well as in other media including CBS, NBC, CNN, BBC, NHK, El Globo, TV Asahi, Al Jazeera, and VOA. Articles discussing FARM instrumentation and/or data have appeared in the *New York Times*, *Washington Post*, *Economist*, *Der Spiegel*, *Discover*, *Popular Science*, *New Scientist*, *USA Today*, *Scientific American*, and many other high-impact publications. Several dozen popular books and textbooks use images or data from FARM instrumentation.

Fig. 11. FARM POLENET unit being deployed on power pole during Hurricane Delta (2020).

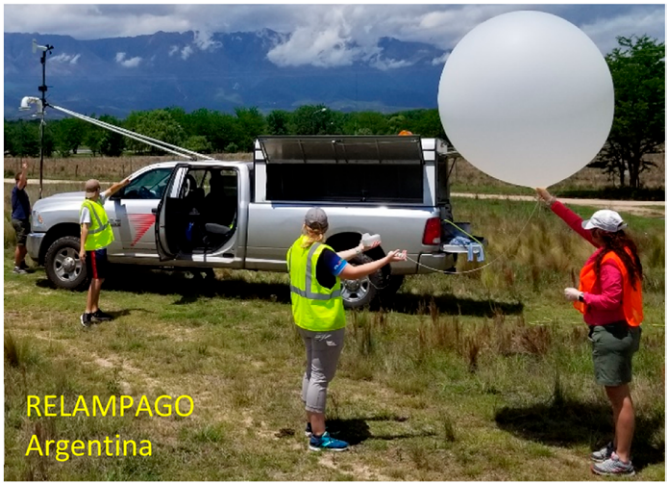

Fig. 12. FARM MQD sounding being launched from an MM which also carries PODNET units.

Unauthenticated | Downloaded 02/01/24 06:03 PM UTC

Data, calibration, displays, field coordination

Calibration and data quality control are critical for radars, especially for reflectivity and dual-polarization fields. System calibrations are conducted by injecting signals through a range of intensities, and by measuring gains and losses of individual and groups of components. Quasi-periodic vertically pointing scans during precipitation provide calibration for Z_{DR}. [Under most circumstances, Z_{DR} is expected to be zero when measured at zenith. Additionally, the average of Z_{DR} through a 360° rotation of a zenith-pointed antenna is expected to be zero even in the presence of strong electrical fields, or wind shear. Deviations from this average are considered error and can be subtracted from raw Z_{DR} fields (see Hubbert et al. 2003).] Intercomparisons with other FARM radars, other research radars, and WSR-88D are made, when possible. Calibrations of MM, PODNET, and POLENET instruments are conducted primarily through intercomparisons among the many FARM systems.

Fig. 13. FARM Mobile Operations and Repair Center (MORC).

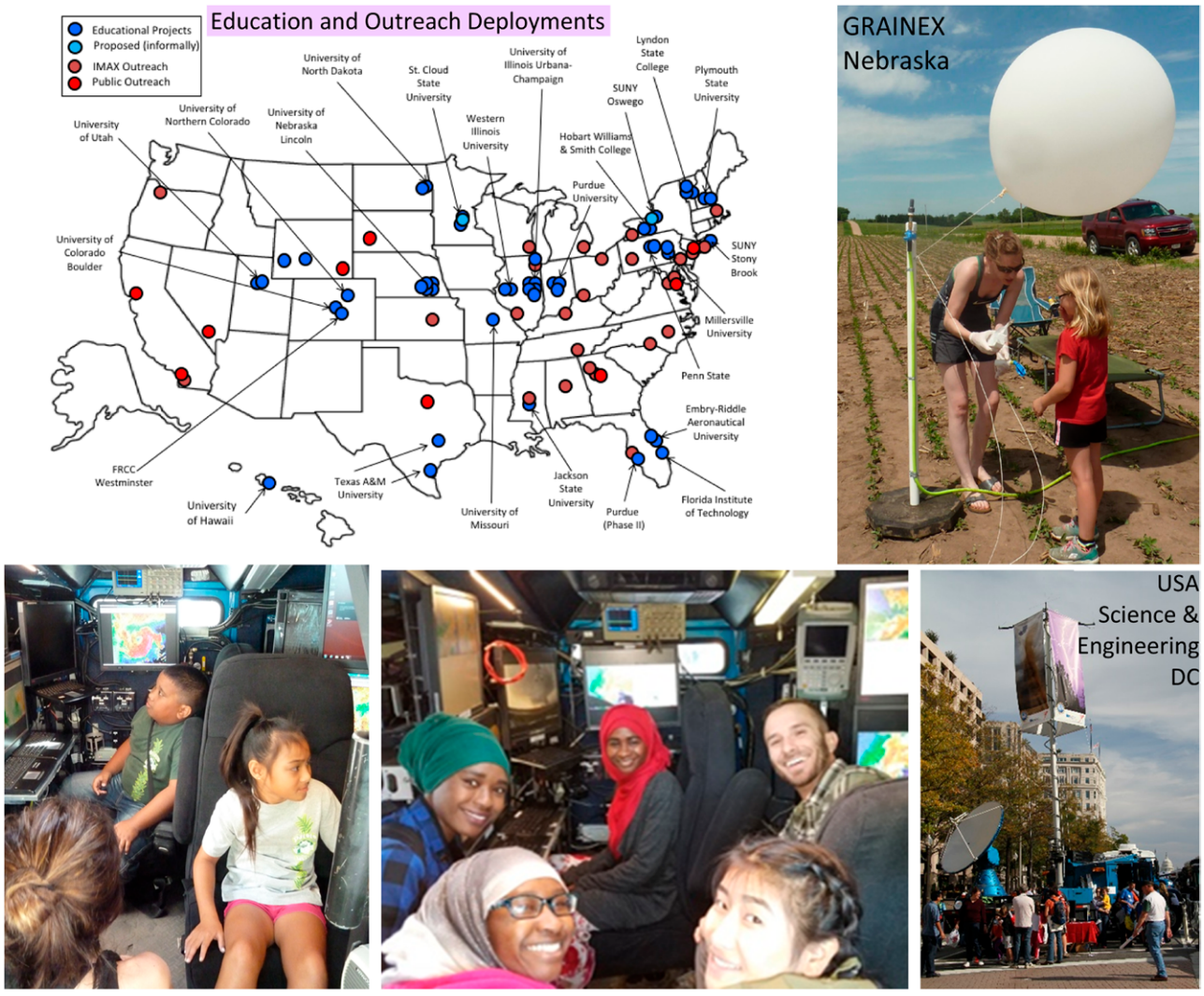

Fig. 14. FARM educational and outreach missions. (clockwise from top left) Map of deployments, ad hoc outreach entraining local children to launch upper-air soundings during the GRAINEX field project, DOW at U.S. Science and Engineering Festival in Washington, D.C., university educational deployment, and outreach with K–12 children.

Unauthenticated | Downloaded 02/01/24 06:03 PM UTC

Data from the FARM, including full time series IQ data from DOWs/COW, frequently require tens of terabytes (TB) of storage capacity, sometimes exceeding 100 TB. Data are stored on relatively inexpensive NAS disk arrays. Physical and cyber data security is achieved through triple redundancy, with one backup copy retained offline and another copy physically remote. Data are typically available through FTP, except for the extremely large time series collections, which are transferable physically.

The FARM facility has developed and maintains a custom suite of radar and instrument data display and field tracking software, the Geographical Unified Radar Utility (GURU) (Fig. 15). This was prototyped for the RELAMPAGO operations center and provides real-time DOW/

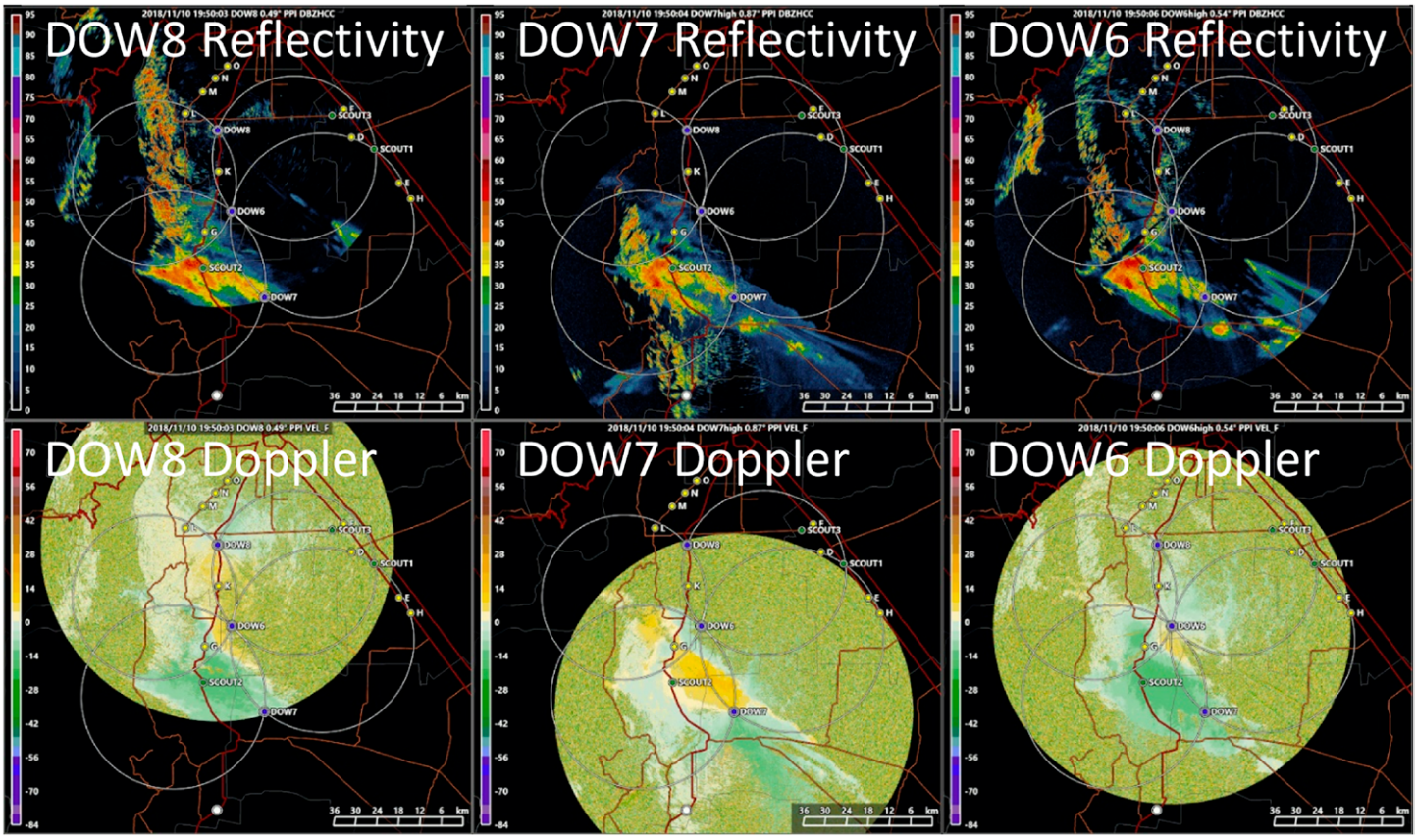

Fig. 15. GURU field data and coordination display. Near-real-time imagery from DOWs/COW is integrated with MM, PODNET, and sounding tracking to aid in mission planning, radar status, and field coordination. This image is from the real-time GURU display in the RELAMPAGO operations center. POD and MM locations are shown relative to DOW reflectivity and Doppler velocity fields.

COW radar displays as well as MM and PODNET deployments, and sounding flight tracks. Radar editing tools for GURU are in development to facilitate enhanced radar data perusal including dealiasing, deglitching, and other data quality functions.

Future FARM instrumentation

The FARM exists to provide cutting-edge, forward-looking instrumentation capabilities for a wide range of meteorological studies and education. Since its inception, the DOW facility, now FARM, has innovated ambitiously, inventing new and broadly useful observational capabilities and techniques (e.g., DOWs themselves, the RSDOW, POLENET, the COW). We envision this inventive mission continuing, including two major innovations to greatly enhance community observational capabilities.

Unauthenticated | Downloaded 02/01/24 06:03 PM UTC

S-band on Wheels (SOW) and SOWNET. Long wavelength, 10-cm (S-band) radars with the ability to penetrate deeply through intense precipitation provide critical operational (WSR-88D) and research capabilities [e.g., S-POL (Lutz et al. 1995); CHILL (Brunkow et al. 2000); NPOL (Petersen and Wolff 2013)].

Stationary or quasi-stationary/transportable radars have design freedom to use large antennas since they are not constrained by road worthiness. The narrow beams and superior precipitation penetrating ability of 10-cm systems allow observations in a variety of intensely precipitating phenomena. Superior Bragg scattering sensitivity permits clear-air observations out to >100-km range. Thus, S-band radars have been core instrumentation for many meteorological studies.

However, since they employ cumbersome, heavy, 8-m diameter antennas, they are very expensive, and difficult and slow to assemble and deploy. Usually, only one radar is deployed, obtaining only single-Doppler measurements.

We envision a new concept, an S-band on Wheels Network (SOWNET) (Fig. 16), comprising multiple quickly deployable, S-band truckborne radars, to address these limitations. A network of four SOWs, SOWNET, will replace a single large S-band 1° beamwidth radar with an array of smaller, 5.5-m (18 ft) antenna, quickly deployable, 1.5° beamwidth truckborne radars. Of course, broader beams result in *potentially* coarser data. But, deployed in arrays, one or more SOWs are nearly always reasonably close to targeted phenomena, so *SOWNET resolution over most of a study area is usually better than that of a single large radar.* We plan to develop a prototype SOW system in the anticipation of deploying future SOWNET.

The key advantages of SOWNET are as follows:

- 1, 2, 3, or 4 SOWs can comprise a SOWNET deployment, customizing for small and large missions
- Resolution resulting from a few SOWs is better than a single large radar
- 5.5-m (18 ft) diameter antennas: <1/2 sail area, <1/2 weight, compared to 1.0° 8-m (26 ft) diameter antennas, reducing power needs and setup time
- SOWs can be assembled with a crew of three, in ~6 h
- Total time to deploy entire SOWNET array = ~5 days
- SOWNET entire network deployment is <1/2 the cost to deploy compared to S-POL, based on much reduced staffing needs and total setup time

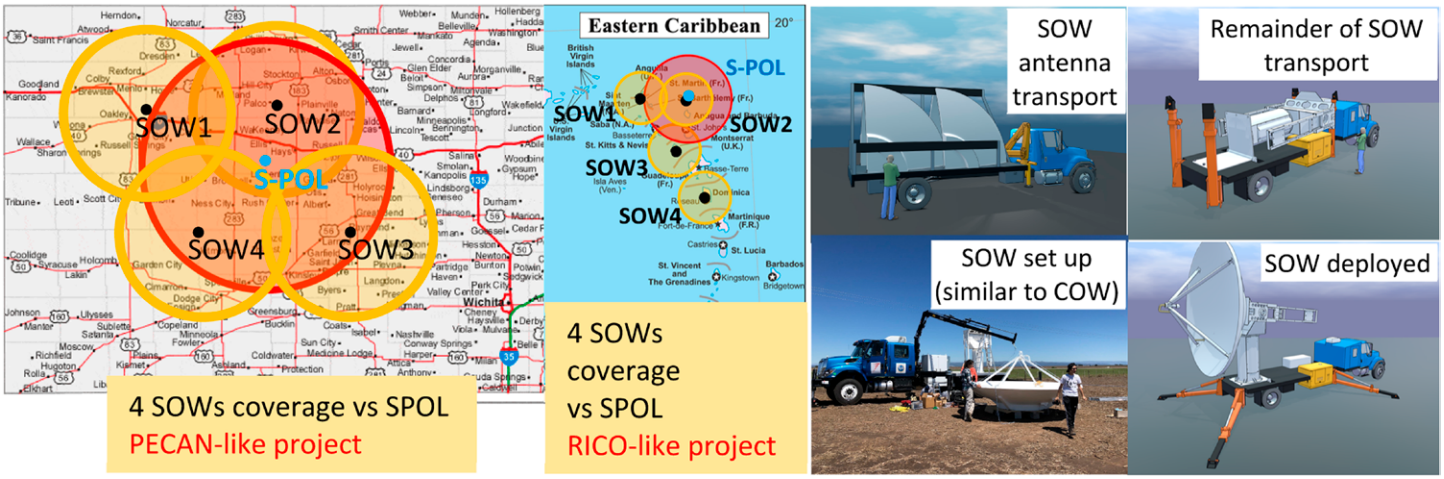

Fig. 16. Comparison of SOWNET and SPOL radar coverage in hypothetical (left) PECAN- and (center) RICO-type studies. Red and orange circles enclose regions with <1.7-km beamwidth (100-km range from S-POL, 67-km range from any of the SOWs). SOWNET provides greater surveillance area. Much of the yellow-shaded areas are within SOWNET multiple-Doppler vector wind coverage. (right) SOW setup requires ~6 h, which is much quicker and less expensive than larger S-band radars.

Unauthenticated | Downloaded 02/01/24 06:03 PM UTC

- SOWs can be operated by lightly trained student crews
- SOWNET arrays can be polygons or quasi linear, and can change during a project
- Reliability is enhanced by eliminating single points of failure; if one SOW breaks, others in the network still provide multiradar coverage
- SOWNET is automatically multiple-Doppler
- Each SOW provides independent dual-polarization observations
- SOWNET will employ DPDF technology to scan twice as fast as current large radars
- SOWNET will employ dual 1-MW transmitters, resulting in greater sensitivity in the clear-air boundary layer compared to existing radars which employ single transmitters

Bistatic Adaptable Radar Network. While DOWs have provided targeted multiple-Doppler vector wind observations for myriad projects, multiple-Doppler deployments remain difficult and expensive.

Bistatic systems (e.g., Wurman et al. 1993; Wurman 1994; Protat and Zawadzki 1999; Friedrich et al. 2000; Satoh and Wurman 2003), particularly mobile units, offer an inexpensive logistically easier capability to observe 3D vector wind fields. They comprise a traditional transmitting and scanning radar paired with one to many remotely deployed receivers with nonscanning low- to medium-gain antennas. Vector winds are calculated from simultaneous measurements in the native coordinate system of the transmitting/receiving radars (no spatial or temporal interpolation required). Bistatic receivers use small antennas, have no expensive transmitters, and can be deployed similarly to PODNET units or carried on small vehicles like MM.

We plan to incorporate a network of MQD bistatic receivers, Bistatic Adaptable Radar Network (BARN), integrated with SOWs, DOWs, and COW, to provide critical vector wind fields. This will form the backbone for many future research projects requiring dual-polarimetric, near-ground, fine-scale, vector wind observations (Fig. 17).

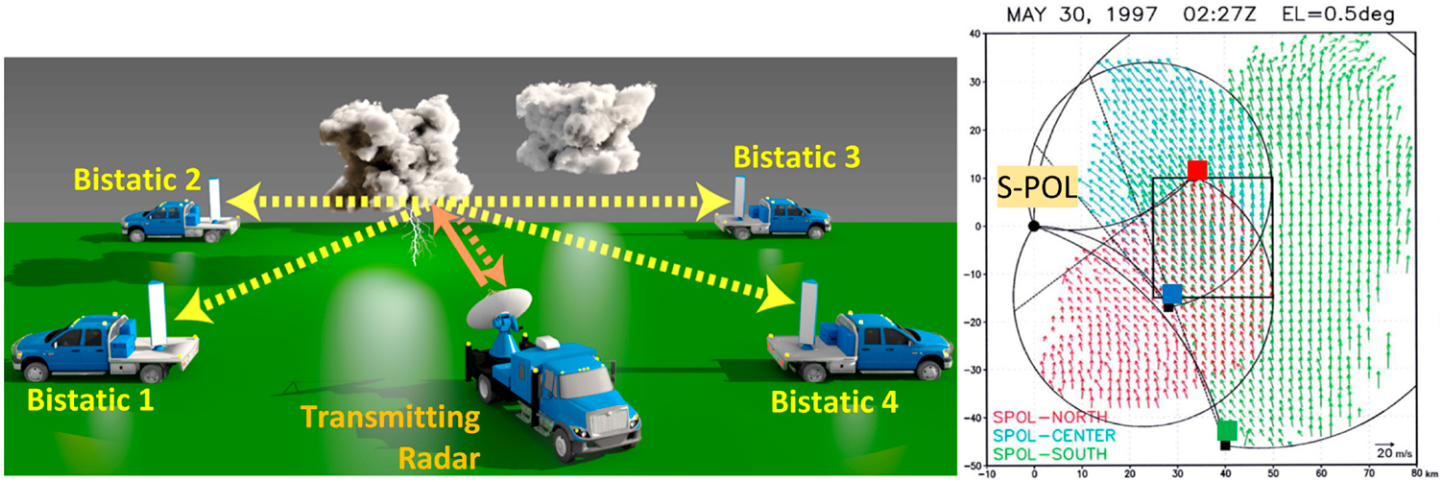

Fig. 17. (left) Schematic mobile bistatic network with four receiving antennas and one transmitting radar. The transmitting radar is, in this example, a DOW or SOW, but can be a stationary radar (e.g., S-POL). The four receiving antennas are on the back of pickup trucks, but can be deployed similarly to Pods. The transmitting and receiving radars can be moved like MMs to optimize coverage and vector wind retrievals as phenomena move/evolve. As the DOW/SOW transmits and scans, the pulses in its narrow radar beam (orange arrow) are scattered from hydrometeors, dust, etc. Some of that scattered energy (dashed yellow arrows) is received by the passive antennas, as well as the by the DOW/SOW antenna (dashed orange arrow). Three-dimensional vector wind fields are calculated from these various Doppler measurements. (right) An example of vector wind retrievals from a bistatic network. In this example, there was one transmitting radar (S-POL) and three bistatic receivers (solid squares). The colored vectors depict the retrievals using data from the north (red), central (blue), and southern (green) bistatic receivers. Arcs depict the bistatic dual-Doppler lobes with the transmitting radar. The square outline encloses an overdetermined analysis domain (image adapted from Satoh and Wurman 2003).

Unauthenticated | Downloaded 02/01/24 06:03 PM UTC

The key features of BARN are as follows:

- BARN enables multiple-Doppler vector wind measurements over targeted regions.
- While SOWNET is providing moderate-resolution multiple-Doppler measurements, BARN provides finer-scale and/or customized measurements over smaller domains.
- BARN units will be configured to couple with different SOWS, COW, or DOWs. Only the receiver front ends and antennas are frequency specific.
- BARN units will be stationary, deployed for the duration of a project, or mobile.
- Stationary BARN units will be unattended, low power, and logistically similar to deployable weather stations.
- Highly redundant BARN units provide extreme reliability of multiple-Doppler operations.
- BARN units are <1/10 the cost of scanning transmitting radars.
- BARN receiving antennas will be designed with different characteristics. These will include previously used low-gain systems optimized to sample broad areas of precipitation, but unable to observe clear-air nonprecipitating regions., Medium-gain systems, perhaps slowly scanning or switching, which can obtain vector wind measurement in the nonprecipitating boundary layer will be designed. Different configurations will be optimized for different observational needs.

Summary

Since 1995 the DOWs and other instrumentation comprising FARM have facilitated a broad and diverse range of observational studies, education, and outreach. DOWs in particular have facilitated a new observational paradigm for many meteorological projects, and are frequently used in conjunction with other FARM systems including PODNET, MMs, disdrometers, and POLENET. The extensive array of FARM instrumentation, comprising four MQD radars, a fleet of MM, PODNET, POLENET, soundings, disdrometers, the MORC, and future systems, will continue to be the backbone of many major research studies, often complemented by additional instrumentation such as Lidars, unmanned aerial systems (UAS), other MQD radars, MM, manned research aircraft, and QD weather stations [e.g., UAS in VORTEX2 (Riganti and Houston 2017), lidar and multiple aircraft in PECAN (Geerts et al. 2017)]. FARM instrumentation has been designed and operated with ease of use, student operability, and low cost in mind.

From 2008 to 2019 these facilities were supported by and available through the Lower Atmospheric Observing Systems (LAOF) program at the National Science Foundation (NSF). This permitted these systems to be used for not only large field projects (e.g., RELAMPAGO, PECAN, VORTEX2), but a variety of smaller single- to several-investigator studies (e.g., OWLeS, SNOWIE, MASCRAD, ASCII, GRAINEX, OLYMPEX). LAOF also supported frequent educational and extensive outreach deployments, impacting thousands of students, and tens of thousands in the general public. FARM, now managed through the University of Illinois, remains available to researchers and educators by request (see http://farm.atmos.illinois.edu), and it is hoped that methods of support and request, enabling the previously broad and diverse access possible through LAOF, will again be realized. As of the time of writing, projects potentially employing FARM instrumentation to study tornadoes, quasi-linear convective systems, mountain/valley wind systems, convective initiation, New England winter storms, northeastern ice and snow storms, hurricanes, and other phenomena are in various stages of planning.

We expect an active future for FARMing.

Acknowledgments. The FARM comprises observational systems developed, constructed, maintained, and operated over 26-plus years. We thank the literally hundreds of operators, drivers, and other supporters of the dozens of educational and research missions, including Curtis Alexander, Steve

Unauthenticated | Downloaded 02/01/24 06:03 PM UTC

Weygandt, David Dowell, Scott Richardson, Yvette Richardson, Herb Stein, Jerry Straka, and Erik Rasmussen from the early years. We thank the engineers, software engineers, and scientists at the National Center for Atmospheric Research, especially Mitch Randall, Chris Burghart, Eric Loew, Mike Dixon, Jeff Keeler, Jim Wilson, and Dave Carlson, the staff of the Center for Severe Weather Research (CSWR), especially Ling Chan, Justin Walker, Rachel Humphrey, Danny Cheresnick, Jim Marquis, Traeger Meyer, and the many experts in the radar meteorology community who provided wisdom over the years, including Earle Williams, Dave Atlas, Isztar Zawadski, Fredric Fabry, Dusan Zrnić, Dick Doviak, Paul Markowski, and Katja Friedrich. Support for the FARM, its DOW Facility precursor, and its missions was provided by the National Science Foundation, the National Oceanic and Atmospheric Administration, the Department of Energy, the Department of Defense, the U.S. Forest Service, the Discovery Channel, National Geographic, the National Aeronautical and Space Administration, the University of Oklahoma, the University of Illinois, the State of Colorado, and several other sources.

Data availability statement. This paper does not describe any particular datasets. Data from the FARM will be available through the FARM Facility by contacting its managers.

References

Alexander, C. R., and J. Wurman, 2005: The 30 May 1998 Spencer, South Dakota, storm. Part I: The structural evolution and environment of the tornadoes. *Mon. Wea. Rev.*, **133**, 72–97, https://doi.org/10.1175/MWR-2855.1.

Armijo, L., 1969: A theory for the determination of wind and precipitation velocities with Doppler radar. *J. Atmos. Sci.*, **26**, 570–573, https://doi.org/10.1175/1520-0469(1969)026<0570:ATFTDO>2.0.CO;2.

Arnott, N. R., Y. P. Richardson, J. Wurman, and E. M. Rasmussen, 2006: Relationship between a weakening cold front, misocyclones, and cloud development on 10 June 2002 during IHOP. *Mon. Wea. Rev.*, **134**, 311–335, https://doi.org/10.1175/MWR3065.1.

Atkins, N. T., A. McGee, R. Ducharme, R. M. Wakimoto, and J. Wurman, 2012: The LaGrange tornado during VORTEX2. Part II: Photogrammetric analysis of the tornado combined with dual-Doppler radar data. *Mon. Wea. Rev.*, **140**, 2939–2958, https://doi.org/10.1175/MWR-D-11-00285.1.

Atlas, D., Ed., 1990: *Radar in Meteorology.* Amer. Meteor. Soc., 806 pp.

Beck, J. R., J. L. Schroeder, and J. Wurman, 2006: High-resolution dual-Doppler analyses of the 29 May 2001 Kress, Texas, cyclic supercell. *Mon. Wea. Rev.*, **134**, 3125–3148, https://doi.org/10.1175/MWR3246.1.

Bedard, A. J., Jr., and C. Ramzy, 1983: Surface meteorological observations in severe thunderstorms, Part I: Design details of TOTO. *J. Appl. Meteor. Climatol.*, **22**, 911–918, https://doi.org/10.1175/1520-0450(1983)022<0911:SMOIST>2.0.CO;2.

Bell, M. M., and Coauthors, 2015: The Hawaiian Educational Radar Opportunity (HERO). *Bull. Amer. Meteor. Soc.*, **96**, 2167–2181, https://doi.org/10.1175/BAMS-D-14-00126.1.

Biggerstaff, M. I., and Coauthors, 2005: The Shared Mobile Atmospheric Research and Teaching radar: A collaboration to enhance research and teaching. *Bull. Amer. Meteor. Soc.*, **86**, 1263–1274, https://doi.org/10.1175/BAMS-86-9-1263.

Bluestein, H. B., 1983: Surface meteorological observations in severe thunderstorms: Field measurements and design detail of TOTO. *J. Appl. Meteor. Climatol.*, **22**, 919–930, https://doi.org/10.1175/1520-0450(1983)022<0919:SMOIST>2.0.CO;2.

——, and W. P. Unruh, 1989: Observations of the wind field in tornadoes, funnel clouds, and wall clouds with a portable Doppler radar. *Bull. Amer. Meteor. Soc.*, **70**, 1514–1525, https://doi.org/10.1175/1520-0477(1989)070<1514:OOTWFI>2.0.CO;2.

Unauthenticated | Downloaded 07/01/24 06:03 PM UTC

——, and J. H. Golden, 1993: A review of tornado observations. *The Tornado: Its Structure, Dynamics, Prediction and Hazards*, *Geophys. Monogr.*, Vol. 79, Amer. Geophys. Union, 19–39.

——, and A. L. Pazmany, 2000: Observations of tornadoes and other convective phenomena with a mobile, 3-mm wavelength, Doppler radar: The spring 1999 field experiment. *Bull. Amer. Meteor. Soc.*, **81**, 2939–2951, https://doi.org/10.1175/1520-0477(2000)081<2939:OOTAOC>2.3.CO;2.

——, ——, J. C. Galloway, and R. E. McIntosh, 1995: Studies of the substructure of severe convective storms using a mobile 3-mm-wavelength Doppler radar. *Bull. Amer. Meteor. Soc.*, **76**, 2155–2170, https://doi.org/10.1175/1520-0477(1995)076<2155:SOTSOS>2.0.CO;2.

Bluestein, H. B., M. M. French, R. L. Tanamachi, S. Frasier, K. Hardwick, F. Junyent, and A. L. Pazmany, 2007: Close-range observations of tornadoes in supercells made with a dual-polarization, X-Band, mobile Doppler radar. *Mon. Wea. Rev.*, **135**, 1522–1543, https://doi.org/10.1175/MWR3349.1.

Bousquet, O., and B. F. Smull, 2003: Airflow and precipitation fields within deep Alpine valleys observed by airborne Doppler radar. *J. Appl. Meteor.*, **42**, 1497–1513, https://doi.org/10.1175/1520-0450(2003)042<1497:AAPFWD>2.0.CO;2.

Bringi, V. N., and V. Chandrasekar, 2001: *Polarimetric Doppler Weather Radar: Principles and Applications*. Cambridge University Press, 636 pp.

——, and D. Zrnić, 2019: Polarization weather radar development from 1970–1995: Personal reflections. *Atmosphere*, **10**, 714, https://doi.org/10.3390/atmos10110714.

Brock, F. V., and P. K. Govind, 1977: Portable automated mesonet in operation. *J. Appl. Meteor. Climatol.*, **16**, 299–310, https://doi.org/10.1175/1520-0450(1977)016<0299:PAMIO>2.0.CO;2.

——, G. Lesins, and R. Walko, 1987: Measurement of pressure and air temperature near severe thunderstorms: An inexpensive and portable instrument. *Extended Abstracts*, *Sixth Symp. on Meteorological Observations and Instrumentation*, New Orleans, LA, Amer. Meteor. Soc., 320–323.

——, K. C. Crawford, R. L. Elliott, G. W. Cuperus, S. J. Stadler, H. L. Johnson, and M. D. Eilts, 1995: The Oklahoma Mesonet: A technical overview. *J. Atmos. Oceanic Technol.*, **12**, 5–19, https://doi.org/10.1175/1520-0426(1995)012<0005:TOMATO>2.0.CO;2.

Browning, K. A., and R. Wexler, 1968: The determination of kinematic properties of a wind field using Doppler radar. *J. Appl. Meteor.*, **7**, 105–113, https://doi.org/10.1175/1520-0450(1968)007<0105:TDOKPO>2.0.CO;2.

Brunkow, D., V. N. Bringi, P. C. Kennedy, S. A. Rutledge, S. V. Chandrasekar, E. A. Mueller, and R. K. Bowie, 2000: A description of the CSU–CHILL national radar facility. *J. Atmos. Oceanic Technol.*, **17**, 1596–1608, https://doi.org/10.1175/1520-0426(2000)017<1596:ADOTCC>2.0.CO;2.

Burgess, D. W., M. A. Magsig, J. Wurman, D. C. Dowell, and Y. Richardson, 2002: Radar observations of the 3 May 1999 Oklahoma City tornado. *Wea. Forecasting*, **17**, 456–471, https://doi.org/10.1175/1520-0434(2002)017<0456:ROOTMO>2.0.CO;2.

Byko, Z., P. Markowski, Y. Richardson, J. Wurman, and E. Adlerman, 2009: Descending reflectivity cores in supercell thunderstorms observed by mobile radars and in a high-resolution numerical simulation. *Wea. Forecasting*, **24**, 155–186, https://doi.org/10.1175/2008WAF2222116.1.

Carbone, R. E., M. J. Carpenter, and C. D. Burghart, 1985: Doppler radar sampling limitations in convective storms. *J. Atmos. Oceanic Technol.*, **2**, 357–361, https://doi.org/10.1175/1520-0426(1985)002<0357:DRSLIC>2.0.CO;2.

Casey, S. C., 2011: *Tornado Alley.* Giant Screen Films–Graphic Films, 43 min.

Doviak, R. J., and D. S. Zrnić, 1984: *Doppler Radar and Weather Observations*. 1st ed. Academic Press, 470 pp.

Fabry, F., 2015: *Radar Meteorology: Principles and Practice*. Cambridge University Press, 276 pp.

Fink, D. G., 1945, The SCR-584 radar: Part I. *Electronics*, November, 104–109.

Foote, G. B., and J. C. Fankhauser, 1973: Airflow and moisture budget beneath a northeast Colorado hailstorm. *J. Appl. Meteor. Climatol.*, **12**, 1330–1353, https://doi.org/10.1175/1520-0450(1973)012<1330:AAMBBA>2.0.CO;2.

Frame, J., P. Markowski, Y. Richardson, J. Straka, and J. Wurman, 2009: Polarimetric and dual-Doppler radar observations of the Lipscomb County, Texas, supercell thunderstorm on 23 May 2002. *Mon. Wea. Rev.*, **137**, 544–561, https://doi.org/10.1175/2008MWR2425.1.

Friedrich, K., M. Hagen, and P. Meischner, 2000: Vector wind field determination by bistatic multiple-Doppler radar. *Phys. Chem. Earth*, **25B**, 1205–1208, https://doi.org/10.1016/S1464-1909(00)00179-9.

——, D. E. Kingsmill, C. Flamant, H. V. Murphey, and R. M. Wakimoto, 2008: Kinematic and moisture characteristics of a nonprecipitating cold front observed during IHOP. Part II: Alongfront structures. *Mon. Wea. Rev.*, **136**, 3796–3821, https://doi.org/10.1175/2008MWR2360.1.

——, E. Kalina, F. Masters, and C. Lopez, 2013: Drop-size distributions in thunderstorms measured by optical disdrometers during VORTEX2. *Mon. Wea. Rev.*, **141**, 1182–1203, https://doi.org/10.1175/MWR-D-12-00116.1.

Fujita, T. T., 1965: Formation and steering mechanisms of tornado cyclones and associated hook echoes. *Mon. Wea. Rev.*, **93**, 67–78, https://doi.org/10.1175/1520-0493(1965)093<0067:FASMOT>2.3.CO;2.

——, 1981: Tornadoes and downbursts in the context generalized planetary scales. *J. Atmos. Sci.*, **38**, 1511–1534, https://doi.org/10.1175/1520-0469(1981)038<1511:TADITC>2.0.CO;2.

Gao, J., M. Xue, A. Shapiro, and K. K. Droegemeier, 1999: A variational method for the analysis of three-dimensional wind fields from two Doppler radars. *Mon. Wea. Rev.*, **127**, 2128–2142, https://doi.org/10.1175/1520-0493(1999)127<2128:AVMFTA>2.0.CO;2.

Geerts, B., and Coauthors, 2013: The AgI Seeding Cloud Impact Investigation (ASCII) campaign 2012: Overview and preliminary results. *J. Wea. Modif.*, **45**, 24–43, http://journalofweathermodification.org/index.php/JWM/article/view/121/.

——, and Coauthors, 2017: The 2015 Plains Elevated Convection At Night (PECAN) field project. *Bull. Amer. Meteor. Soc.*, **98**, 767–786, https://doi.org/10.1175/BAMS-D-15-00257.1.

Hildebrand, P. H., and Coauthors, 1996: The ELDORA/ASTRAIA airborne Doppler weather radar: High-resolution observations from TOGA COARE. *Bull. Amer. Meteor. Soc.*, **77**, 213–232, https://doi.org/10.1175/1520-0477(1996)077<0213:TEADWR>2.0.CO;2.

Horel, J., and Coauthors, 2002: MESOWEST: Cooperative mesonets in the western United States. *Bull. Amer. Meteor. Soc.*, **83**, 211–226, https://doi.org/10.1175/1520-0477(2002)083<0211:MCMITW>2.3.CO;2.

Houze, R. A., Jr., B. F. Smull, and P. Dodge, 1990: Mesoscale organization of springtime rainstorms in Oklahoma. *Mon. Wea. Rev.*, **118**, 613–654, https://doi.org/10.1175/1520-0493(1990)118<0613:MOOSRI>2.0.CO;2.

——, and Coauthors, 2017: The Olympic Mountains Experiment (OLYMPEX). *Bull. Amer. Meteor. Soc.*, **98**, 2167–2188, https://doi.org/10.1175/BAMS-D-16-0182.1.

Hubbert, J. C., V. N. Bringi, and D. Brunkow, 2003: Studies of the polarimetric covariance matrix. Part I: Calibration methodology. *J. Atmos. Oceanic Technol.*, **20**, 696–706, https://doi.org/10.1175/1520-0426(2003)20<696:SOTPCM>2.0.CO;2.

Junyent, F., V. Chandrasekar, D. McLaughlin, E. Insanic, and N. Bharadwaj, 2010: The CASA integrated project 1 networked radar system. *J. Atmos. Oceanic Technol.*, **27**, 61–78, https://doi.org/10.1175/2009JTECHA1296.1.

Keeler, R. J., and C. L. Frush, 1983: Rapid scan Doppler radar development considerations, Part II: Technology assessment. Preprints, *21st Conf. on Radar Meteorology*, Edmonton, AB, Canada, Amer. Meteor. Soc., 284–290.

——, B. W. Lewis, and G. R. Gray, 1989: Description of NCAR/FOF CP-2 meteorological Doppler radar. Preprints, *24th Conf. on Radar Meteorology*, Tallahassee, FL, Amer. Meteor. Soc., 589–592.

Kosiba, K. A., 2009: A comparison of radar observations to real data simulations of axisymmetric tornadoes. Ph.D. dissertation, Dept. of Earth and Atmospheric Sciences, Purdue University, 126 pp.

——, and J. Wurman, 2009: High resolution and in-situ observations in the hurricane boundary layer: Ike and Gustav. *34th Conf. on Radar Meteorology,* Williamsburg, VA, Amer. Meteor. Soc., 12A.1, https://ams.confex.com/ams/34Radar/webprogram/Paper156151.html.

Unauthenticated | Downloaded 02/01/24 06:03 PM UTC

——, and ——, 2010: The three-dimensional axisymmetric wind field structure of the Spencer, South Dakota, 1998 tornado. *J. Atmos. Sci.*, **67**, 3074–3083, https://doi.org/10.1175/2010JAS3416.1.

——, and ——, 2013: The three-dimensional structure and evolution of a tornado boundary layer. *Wea. Forecasting*, **28**, 1552–1561, https://doi.org/10.1175/WAF-D-13-00070.1.

——, and ——, 2014: Fine-scale dual-Doppler analysis of hurricane boundary layer structures in Hurricane Frances (2004) at landfall. *Mon. Wea. Rev.*, **142**, 1874–1891, https://doi.org/10.1175/MWR-D-13-00178.1.

——, and ——, 2016a: The TWIRL (Tornado Winds from In-situ and Radars at Low-level) Project. *28th Conf. on Severe Local Storms,* Portland, OR, Amer. Meteor. Soc., 4.2, https://ams.confex.com/ams/28SLS/webprogram/Paper302011.html.

——, and ——, 2016b: PECAN: Characteristics of potentially severe wind producing nocturnal MCSs. *98th AMS Annual Meeting*, Austin, TX, Amer. Meteor. Soc., 3.2, https://ams.confex.com/ams/98Annual/webprogram/Paper335012.html.

——, and ——, 2018: Mapping of winds in landfalling Irma from two DOWs and several pods deployed near Naples, Florida. *33rd Conf. on Hurricanes and Tropical Meteorology*, Ponte Vedra, FL, Amer. Meteor. Soc., 4D.7, https://ams.confex.com/ams/33HURRICANE/webprogram/Paper340238.html.

——, and Coauthors, 2012: Mobile radar observations and damage assessment of the 24 May 2011, Canton Lake, OK tornado. *26th Conf. on Severe Local Storms,* Nashville, TN, Amer. Meteor. Soc., 102, https://ams.confex.com/ams/26SLS/webprogram/Paper211754.html.

——, J. Wurman, F. J. Masters, and P. Robinson, 2013a: Mapping of near-surface winds in Hurricane Rita using finescale radar, anemometer and land-use data. *Mon. Wea. Rev.*, **141**, 4337–4349, https://doi.org/10.1175/MWR-D-12-00350.1.

——, ——, Y. Richardson, P. Markowski, P. Robinson, and J. Marquis, 2013b: Genesis of the Goshen County, Wyoming, tornado on 5 June 2009 during VORTEX2. *Mon. Wea. Rev.*, **141**, 1157–1181, https://doi.org/10.1175/MWR-D-12-00056.1.

——, ——, K. Knupp, K. Pennington, and P. Robinson, 2020a: Ontario Winter Lake-effect Systems (OWLeS): Bulk characteristics and kinematic evolution of misovortices in long-lake-axis-parallel snowbands. *Mon. Wea. Rev.*, **148**, 131–157, https://doi.org/10.1175/MWR-D-19-0182.1.

——, ——, and P. Robinson, 2020b: Low-level winds in tornadoes. *Severe Local Storms Symp.*, Boston, MA, Amer. Meteor. Soc., 1.2, https://ams.confex.com/ams/2020Annual/meetingapp.cgi/Paper/369823.

Kristovich, D., and Coauthors, 2017: The Ontario Winter Lake-effect Systems field campaign: Scientific and educational adventures to further our knowledge and prediction of lake-effect storms. *Bull. Amer. Meteor. Soc.*, **98**, 315–332, https://doi.org/10.1175/BAMS-D-15-00034.1.

Kumjian, M. R., and A. V. Ryzhkov, 2008: Polarimetric signatures in supercell thunderstorms. *J. Appl. Meteor. Climatol.*, **47**, 1940–1961, https://doi.org/10.1175/2007JAMC1874.1.

Lee, J. L., T. Samaras, and C. Young, 2004: Pressure measurements at the ground in an F-4 tornado. *22nd Conf. on Severe Local Storms*. Hyannis, MA, Amer. Meteor. Soc., 15.3, https://ams.confex.com/ams/11aram22sls/techprogram/paper_81700.htm.

Lee, W.-C., and J. Wurman, 2005: Diagnosed three-dimensional axisymmetric structure of the Mulhall tornado on 3 May 1999. *J. Atmos. Sci.*, **62**, 2373–2393, https://doi.org/10.1175/JAS3489.1.

——, F. D. Marks, and R. E. Carbone, 1994: Velocity track display—A technique to extract real-time tropical cyclone circulations using a single airborne Doppler radar. *J. Atmos. Oceanic Technol.*, **11**, 337–356, https://doi.org/10.1175/1520-0426(1994)011<0337:VTDTTE>2.0.CO;2.

Lorsolo, S., J. L. Schroeder, P. Dodge, and F. Marks, 2008: An observational study of hurricane boundary layer small-scale coherent structures. *Mon. Wea. Rev.*, **136**, 2871–2893, https://doi.org/10.1175/2008MWR2273.1.

Lutz, J., P. Johnson, B. Lewis, E. Loew, M. Randall, and J. VanAndel, 1995: NCAR's S-POL portable polarimetric C-band radar. Preprints, *Ninth Symp. on Meteorological Observations and Instrumentation,* Charlotte, NC, Amer. Meteor. Soc., 408–410.

Markowski, P. M., J. M. Straka, and E. N. Rasmussen, 2002: Direct surface thermodynamic observations within the rear-flank downdrafts of nontornadic and tornadic supercells. *Mon. Wea. Rev.*, **130**, 1692–1721, https://doi.org/10.1175/1520-0493(2002)130<1692:DSTOWT>2.0.CO;2.

——, and Coauthors, 2012a: The pretornadic phase of the Goshen County, Wyoming, supercell of 5 June 2009 intercepted by VORTEX2. Part I: Evolution of kinematic and surface thermodynamic fields. *Mon. Wea. Rev.*, **140**, 2887–2915, https://doi.org/10.1175/MWR-D-11-00336.1.

——, and Coauthors, 2012b: The pretornadic phase of the Goshen County, Wyoming, supercell of 5 June 2009 intercepted by VORTEX2. Part II: Intensification of low-level rotation. *Mon. Wea. Rev.*, **140**, 2916–2938, https://doi.org/10.1175/MWR-D-11-00337.1.

——, T. P. Hatlee, and Y. P. Richardson, 2018a: Tornadogenesis in the 12 May 2010 supercell thunderstorm intercepted by VORTEX2 near Clinton, Oklahoma. *Mon. Wea. Rev.*, **146**, 3623–3650, https://doi.org/10.1175/MWR-D-18-0196.1.

——, Y. P. Richardson, S. J. Richardson, and A. Petersson, 2018b: Above-ground thermodynamic observations in convective storms from balloonborne probes acting as pseudo-Lagrangian drifters. *Bull. Amer. Meteor. Soc.*, **99**, 711–724, https://doi.org/10.1175/BAMS-D-17-0204.1.

Marquis, J. N., Y. P. Richardson, and J. M. Wurman, 2007: Kinematic observations of misocyclones along boundaries during IHOP. *Mon. Wea. Rev.*, **135**, 1749–1768, https://doi.org/10.1175/MWR3367.1.

——, ——, ——, and P. Markowski, 2008: Single- and dual-Doppler analysis of a tornadic vortex and surrounding storm-scale flow in the Crowell, Texas, supercell of 30 April 2000. *Mon. Wea. Rev.*, **136**, 5017–5043, https://doi.org/10.1175/2008MWR2442.1.

——, ——, P. Markowski, D. Dowell, and J. Wurman, 2012: Tornado maintenance investigated with high-resolution dual-Doppler and EnKF analysis. *Mon. Wea. Rev.*, **140**, 3–27, https://doi.org/10.1175/MWR-D-11-00025.1.

Marshall, J. S., and W. Mc. K. Palmer, 1948: The distribution of raindrops with size. *J. Meteor.*, **5**, 165–166, https://doi.org/10.1175/1520-0469(1948)005<0165:TDORWS>2.0.CO;2.

Masters, F. J., H. W. Tieleman, and J. A. Balderrama, 2010: Surface wind measurements in three Gulf Coast hurricanes of 2005. *J. Wind Eng. Ind. Aerodyn.*, **98**, 533–547, https://doi.org/10.1016/j.jweia.2010.04.003.

Miller, R. L., C. L. Ziegler, and M. I. Biggerstaff, 2020: Seven-Doppler radar and in situ analysis of the 25–26 June 2015 Kansas MCS during PECAN. *Mon. Wea. Rev.*, **148**, 211–240, https://doi.org/10.1175/MWR-D-19-0151.1.

Milrad, S., and C. Herbster, 2017: Mobile radar as an undergraduate education and research tool: The ERAU C-BREESE field experience with the Doppler on Wheels. *Bull. Amer. Meteor. Soc.*, **98**, 1931–1948, https://doi.org/10.1175/BAMS-D-15-00281.1.

Morrison, I., S. Businger, F. Marks, P. Dodge, and J. A. Businger, 2005: An observational case for the prevalence of roll vortices in the hurricane boundary layer. *J. Atmos. Sci.*, **62**, 2662–2673, https://doi.org/10.1175/JAS3508.1.

Mueller, S., C. S. Morse, D. Garvey, R. Barron, D. Albo, and P. Prestopnik, 2004: Juneau airport wind hazard alert system display products. *11th Conf. on Aviation, Range, and Aerospace Meteorology*, Hyannis, MA, Amer. Meteor. Soc., P4.7, https://ams.confex.com/ams/11aram22sls/techprogram/paper_81647.htm.

Mulholland, J. P., J. Frame, S. W. Nesbitt, S. M. Steiger, K. A. Kosiba, and J. Wurman, 2017: Observations of misovortices within a long-lake-axis-parallel lake-effect snowband during the OWLeS project. *Mon. Wea. Rev.*, **145**, 3265–3291, https://doi.org/10.1175/MWR-D-16-0430.1.

NSF, 2015: Mission impossible? New England's snowstorm 'bomb' from inside a Doppler-on-Wheels. Accessed 12 January 2021, www.nsf.gov/discoveries/disc_summ.jsp?cntn_id=134156.

NSSL, 2021: Research tools: Mobile radar. Accessed 12 January 2021, www.nssl.noaa.gov/tools/radar/mobile/.

Nesbitt, S. N., and Coauthors, 2021: A storm safari in subtropical South America: Proyecto RELAMPAGO. *Bull. Amer. Meteor. Soc.*, https://doi.org/10.1175/BAMS-D-20-0029.1, in press.

Unauthenticated | Downloaded 02/01/24 06:03 PM UTC

Niziol, T. A., W. R. Snyder, and J. S. Waldstreicher, 1995: Winter weather forecasting throughout the eastern United States. Part IV: Lake-effect snow. *Wea. Forecasting*, **10**, 61–77, https://doi.org/10.1175/1520-0434(1995)010<0061:WWFTTE>2.0.CO;2.

OFCM, 2017: WSR-88D meteorological observations: Part C—WSR-88D products and algorithms. OFCM Rep. FCM-H11C-2017, 394 pp., www.icams-portal.gov/publications/fmh/FMH11/fmh11partC.pdf.

Pazmany, A. L., J. B. Mead, H. B. Bluestein, J. C. Snyder, and J. B. Houser, 2013: A mobile rapid-scanning X-band polarimetric (RaXPol) Doppler radar system. *J. Atmos. Oceanic Technol.*, **30**, 1398–1413, https://doi.org/10.1175/JTECH-D-12-00166.1.

Petersen, W. A., and D. B. Wolff, 2013: The NASA Polarimetric Radar (NPOL). NASA Doc., 11 pp., https://ntrs.nasa.gov/archive/nasa/casi.ntrs.nasa.gov/20140010713.pdf.

——, and Coauthors, 2004: The UAH-NSSTC/WHNT ARMOR C-band dual-polarimetric radar: A unique collaboration in research, education and technology transfer. *32nd Conf. on Radar Meteorology*, Albuquerque, NM, Amer. Meteor. Soc., 12R.4, https://ams.confex.com/ams/32Rad11Meso/techprogram/paper_96524.htm.

Protat, A., and I. Zawadzki, 1999: A variational method for real-time retrieval of three-dimensional wind field from multiple-Doppler bistatic radar network data. *J. Atmos. Oceanic Technol.*, **16**, 432–449, https://doi.org/10.1175/1520-0426(1999)016<0432:AVMFRT>2.0.CO;2.

Ralph, F. M., and Coauthors, 1999: The California Land-falling Jets Experiment (CALJET): Objectives and design of a coastal atmosphere-ocean observing system deployed during a strong El Nino. Preprints, *Third Symp. on Integrated Observing Systems*, Dallas, TX, Amer. Meteor. Soc., 78–81.

Rappin, E., and Coauthors, 2021: The Great Plains Irrigation Experiment (GRAINEX). *Bull. Amer. Meteor. Soc.*, https://doi.org/10.1175/BAMS-D-20-0041.1, in press.

Rasmussen, E. N., J. M. Straka, R. Davies-Jones, C. A. Doswell, III, F. H. Carr, M. D. Eilts, and D. R. MacGorman, 1994: Verification of the origins of rotation in tornadoes experiment: VORTEX. *Bull. Amer. Meteor. Soc.*, **75**, 995–1006, https://doi.org/10.1175/1520-0477(1994)075<0995:VOTOOR>2.0.CO;2.

Rauber, R. M., and S. W. Nesbitt, 2018: *Radar Meteorology: A First Course*. John Wiley and Sons, 166 pp.

Ray, P. S., R. J. Doviak, G. B. Walker, D. Sirmans, J. Carter, and B. Bumgarner, 1975: Dual-Doppler observation of a tornadic storm. *J. Appl. Meteor. Climatol.*, **14**, 1521–1530, https://doi.org/10.1175/1520-0450(1975)014<1521:DDOOAT>2.0.CO;2.

Refan, M., H. Hangan, and J. Wurman, 2014: Reproducing tornadoes in laboratory using proper scaling. *J. Wind Eng. Ind. Aerodyn.*, **135**, 136–148, https://doi.org/10.1016/j.jweia.2014.10.008.

Richardson, Y., P. Markowski, J. Verlinde, and J. Wurman, 2008: Integrating classroom learning and research: The Pennsylvania Area Mobile Radar Experiment (PAMREX). *Bull. Amer. Meteor. Soc.*, **89**, 1097–1101, https://doi.org/10.1175/1520-0477-89.8.1091.

Riganti, C. J., and A. L. Houston, 2017: Rear-flank outflow dynamics and thermodynamics in the 10 June 2010 Last Chance, Colorado, supercell. *Mon. Wea. Rev.*, **145**, 2487–2504, https://doi.org/10.1175/MWR-D-16-0128.1.

Rinehart, R. E., 1990: *Radar for Meteorologists*. 1st ed. University of North Dakota, 218 pp.

Rust, W. D., D. W. Burgess, R. A. Maddox, L. C. Showell, T. C. Marshall, and D. K. Lauritsen, 1990: Testing a mobile version of a cross-chain LORAN atmospheric (M-CLASS) chain sounding system. *Bull. Amer. Meteor. Soc.*, **71**, 173–180, https://doi.org/10.1175/1520-0477(1990)071<0173:TAMVOA>2.0.CO;2.

Satoh, S., and J. Wurman, 2003: Accuracy of wind fields observed by a bistatic Doppler radar network. *J. Atmos. Oceanic Technol.*, **20**, 1077–1091, https://doi.org/10.1175/1520-0426(2003)020<1077:AOWFOB>2.0.CO;2.

Schroeder, J. L., and C. C. Weiss, 2008: Integrating research and education through measurement and analysis. *Bull. Amer. Meteor. Soc.*, **89**, 793–804, https://doi.org/10.1175/2008BAMS2287.1.

——, W. S. Burgett, K. B. Haynie, I. Sonmez, G. D. Skwira, A. L. Doggett, and J. W. Lipe, 2005: The West Texas mesonet: A technical overview. *J. Atmos. Oceanic Technol.*, **22**, 211–222, https://doi.org/10.1175/JTECH-1690.1.

Schultz, D. M., and Coauthors, 2002: Understanding Utah winter storms: The Intermountain Precipitation Experiment. *Bull. Amer. Meteor. Soc.*, **83**, 189–210, https://doi.org/10.1175/1520-0477(2002)083<0189:UUWSTI>2.3.CO;2.

Schumacher, R., and Coauthors, 2021: Convective-storm environments in subtropical South America from high-frequency soundings during RELAMPAGO-CACTI. *Mon. Wea. Rev.*, **149**, 1439–1458, https://doi.org/10.1175/MWR-D-20-0293.1.

Shapiro, A., C. K. Potvin, and J. Gao, 2009: Use of a vertical vorticity equation in variational dual-Doppler wind analysis. *J. Atmos. Oceanic Technol.*, **26**, 2089–2106, https://doi.org/10.1175/2009JTECHA1256.1.

Steiger, S. A., and Coauthors, 2013: Circulations, bounded weak echo regions, and horizontal vortices observed within long-lake-axis-parallel–lake-effect storms by the Doppler on Wheels. *Mon. Wea. Rev.*, **141**, 2821–2840, https://doi.org/10.1175/MWR-D-12-00226.1.

Stout, G. E., and F. A. Huff, 1953: Radar records Illinois tornadogenesis. *Bull. Amer. Meteor. Soc.*, **34**, 281–284, https://doi.org/10.1175/1520-0477-34.6.281.

Straka, J. M., E. N. Rasmussen, and S. E. Fredrickson, 1996: A mobile mesonet for finescale meteorological observations. *J. Atmos. Oceanic Technol.*, **13**, 921–936, https://doi.org/10.1175/1520-0426(1996)013<0921:AMMFFM>2.0.CO;2.

Tessendorf, S. A., and Coauthors, 2019: A transformational approach to winter orographic weather modification research: The SNOWIE project. *Bull. Amer. Meteor. Soc.*, **100**, 71–92, https://doi.org/10.1175/BAMS-D-17-0152.1.

Toth, M., E. Jones, D. Pittman, and D. Solomon, 2011: DOW radar observations of wind farms. *Bull. Amer. Meteor. Soc.*, **92**, 987–995, https://doi.org/10.1175/2011BAMS3068.1.

——, R. J. Trapp, J. Wurman, and K. Kosiba, 2013: Comparison of mobile-radar measurements of tornado intensity with corresponding WSR-88D measurements. *Wea. Forecasting*, **28**, 418–426, https://doi.org/10.1175/WAF-D-12-00019.1.

Trapp, R. J., 2013: *Mesoscale-Convective Processes in the Atmosphere*. Cambridge University Press, 346 pp.

——, D. J. Stensrud, M. C. Coniglio, R. S. Schumacher, M. E. Baldwin, S. Waugh, and D. T. Conlee, 2016: Mobile radiosonde deployments during the Mesoscale Predictability Experiment (MPEX): Rapid and adaptive sampling of upscale convective feedbacks. *Bull. Amer. Meteor. Soc.*, **97**, 329–336, https://doi.org/10.1175/BAMS-D-14-00258.1.

——, D. Hence, K. Kosiba, M. Kumjian, J. Marquis, S. Nesbitt, P. Salio, and J. Wurman, 2020: Multiple-platform, and multiple-Doppler radar observations of a supercell thunderstorm in South America during RELAMPAGO. *Mon. Wea. Rev.*, **148**, 3225–3241, https://doi.org/10.1175/MWR-D-20-0125.1.

UAH, 2021. MAX (Mobile Alabama X-band). Accessed on 12 January 2021, www.nsstc.uah.edu/mips/max/.

Wakimoto, R. M., and V. N. Bringi, 1988: Dual-polarization observations of microbursts associated with intense convection: The 20 July storm during the MIST Project. *Mon. Wea. Rev.*, **116**, 1521–1539, https://doi.org/10.1175/1520-0493(1988)116<1521:DPOOMA>2.0.CO;2.

——, N. T. Atkins, and J. Wurman, 2011: The LaGrange tornado during VORTEX2. Part I: Photogrammetric analysis of the tornado combined with single-Doppler radar data. *Mon. Wea. Rev.*, **139**, 2233–2258, https://doi.org/10.1175/2010MWR3568.1.

——, P. Stauffer, W.-C. Lee, N. T. Atkins, and J. Wurman, 2012: Finescale structure of the LaGrange, Wyoming, tornado during VORTEX2: GBVTD and photogrammetric analyses. *Mon. Wea. Rev.*, **140**, 3397–3418, https://doi.org/10.1175/MWR-D-12-00036.1.

Weckwerth, T. M., T. W. Horst, and J. W. Wilson, 1999: An observational study of the evolution of horizontal convective rolls. *Mon. Wea. Rev.*, **127**, 2160–2179, https://doi.org/10.1175/1520-0493(1999)127<2160:AOSOTE>2.0.CO;2.

——, L. J. Bennett, L. J. Miller, J. V. Baelen, P. D. Girolamo, A. M. Blyth, and T. J. Hertneky, 2014: An observational and modeling study of the processes leading to deep, moist convection in complex terrain. *Mon. Wea. Rev.*, **142**, 2687–2708, https://doi.org/10.1175/MWR-D-13-00216.1.

Unauthenticated | Downloaded 02/01/24 06:03 PM UTC

Weiss, C. C., J. L. Schroeder, J. Guynes, P. S. Skinner, and J. Beck, 2009: The TTUKa mobile Doppler radar: Coordinated radar and in-situ measurements of supercell thunderstorms during Project VORTEX2. *34th Conf. on Radar Meteorology*, Williamsport, VA, Amer. Meteor. Soc., 11B.2, https://ams.confex.com/ams/34Radar/techprogram/paper_155425.htm.

Wilson, J. W., and W. E. Schreiber, 1986: Initiation of convective storms at radar-observed boundary-layer convergence lines. *Mon. Wea. Rev.*, **114**, 2516–2536, https://doi.org/10.1175/1520-0493(1986)114<2516:IOCSAR>2.0.CO;2.

——, R. D. Roberts, C. Kessinger, and J. McCarthy, 1984: Microburst wind structure and evaluation of Doppler radar for airport wind shear detection. *J. Appl. Meteor. Climatol.*, **23**, 898–915, https://doi.org/10.1175/1520-0450(1984)023<0898:MWSAEO>2.0.CO;2.

Winn, W. P., S. J. Hunyady, and G. D. Aulich, 1999: Pressure at the ground in a large tornado. *J. Geophys. Res.*, **104**, 22 067–22 082, https://doi.org/10.1029/1999JD900387.

Wulfmeyer, V., and Coauthors, 2008: The Convective and Orographically Induced Precipitation Study. *Bull. Amer. Meteor. Soc.*, **89**, 1477–1486, https://doi.org/10.1175/1520-0477-89.10.1469.

Wurman, J., 1994: Vector winds from a single transmitter bistatic dual-Doppler radar network. *Bull. Amer. Meteor. Soc.*, **75**, 983–994, https://doi.org/10.1175/1520-0477(1994)075<0983:VWFAST>2.0.CO;2.

——, 2002: The multiple-vortex structure of a tornado. *Wea. Forecasting*, **17**, 473–505, https://doi.org/10.1175/1520-0434(2002)017<0473:TMVSOA>2.0.CO;2.

——, 2003: Multiple-Doppler observations of tornadoes and tornadogenesis from the ROTATE-2003 project. *31st Conf. on Radar Meteorology*, Seattle, WA, Amer. Meteor. Soc., P4A.1, https://ams.confex.com/ams/32BC31R5C/webprogram/Paper63886.html.

——, 2004: High resolution observations of boundary layer structures in Isabel at landfall. *26th Conf. on Hurricanes and Tropical Meteorology*, Miami, FL, Amer. Meteor. Soc., P1.89, https://ams.confex.com/ams/26HURR/webprogram/Paper76440.html.

——, 2008: Preliminary results and report of the ROTATE-2008 radar/in-situ/mobile mesonet experiment. *24th Conf. on Severe Local Storms*, Savannah, GA, Amer. Meteor. Soc., 5.4, https://ams.confex.com/ams/24SLS/webprogram/Paper142200.html.

——, and J. Winslow, 1998: Intense sub-kilometer-scale boundary layer rolls observed in Hurricane Fran. *Science*, **280**, 555–557, https://doi.org/10.1126/science.280.5363.555.

——, and S. Gill, 2000: Finescale radar observations of the Dimmitt, Texas (2 June 1995), tornado. *Mon. Wea. Rev.*, **128**, 2135–2164, https://doi.org/10.1175/1520-0493(2000)128<2135:FROOTD>2.0.CO;2.

——, and M. Randall, 2001: An inexpensive, mobile, rapid-scan radar. *30th Conf. on Radar Meteorology,* Munich, Germany, Amer. Meteor. Soc., P3.4, https://ams.confex.com/ams/30radar/techprogram/paper_21577.htm.

——, and S. Weygandt, 2003: Mobile radar observations of the Big Elk (2002) and Roberts (2003) fires. *Fifth Symp. on Fire and Forest Meteorology*, Orlando, FL, Amer. Meteor. Soc., https://ams.confex.com/ams/FIRE2003/techprogram/paper_65727.htm.

——, and T. Samaras, 2004: Comparison of in-situ pressure and DOW Doppler winds in a tornado and RHI vertical slices through 4 tornadoes during 1996–2004. *22nd Conf. on Severe Local Storms*, Hyannis, MA, Amer. Meteor. Soc., 15.4, https://ams.confex.com/ams/11aram22sls/techprogram/paper_82352.htm.

——, and C. R. Alexander, 2005: The 30 May 1998 Spencer, South Dakota, storm. Part II: Comparison of observed damage and radar-derived winds in the tornadoes. *Mon. Wea. Rev.*, **133**, 97–119, https://doi.org/10.1175/MWR-2856.1.

——, and K. Kosiba, 2013: Finescale radar observations of tornado and mesocyclone structures. *Wea. Forecasting*, **28**, 1157–1174, https://doi.org/10.1175/WAF-D-12-00127.1.

——, and P. Robinson, 2013: Wind speed suppression by large buildings in hurricanes. *36th Conf. on Radar Meteorology*, Breckenridge, CO, Amer. Meteor. Soc., 184, https://ams.confex.com/ams/36Radar/webprogram/Paper229320.html.

——, and K. Kosiba, 2018a: The role of small-scale vortices in enhancing surface winds and damage in Hurricane Harvey (2017). *Mon. Wea. Rev.*, **146**, 713–722, https://doi.org/10.1175/MWR-D-17-0327.1.

——, and ——, 2018b: Fine-scale multiple-Doppler and thermodynamic observations in an eclipse. *98th AMS Annual Meeting*, Austin, TX, Amer. Meteor. Soc., 390, https://ams.confex.com/ams/98Annual/webprogram/Paper340290.html.

——, S. Heckman, and D. Boccippio, 1993: A bistatic multiple-Doppler network. *J. Appl. Meteor. Climatol.*, **32**, 1802–1814, https://doi.org/10.1175/1520-0450(1993)032<1802:ABMDRN>2.0.CO;2.

——, J. Straka, and E. Rasmussen, 1996: Fine-scale Doppler radar observation of tornadoes. *Science*, **272**, 1774–1777, https://doi.org/10.1126/science.272.5269.1774.

——, ——, ——, M. Randall, and A. Zahrai, 1997: Design and deployment of a portable, pencil-beam, pulsed, 3-cm Doppler radar. *J. Atmos. Oceanic Technol.*, **14**, 1502–1512, https://doi.org/10.1175/1520-0426(1997)014<1502:DADOAP>2.0.CO;2.

——, Y. Richardson, C. Alexander, S. Weygandt, and P. F. Zhang, 2007a: Dual-Doppler and single-Doppler analysis of a tornadic storm undergoing mergers and repeated tornadogenesis. *Mon. Wea. Rev.*, **135**, 736–758, https://doi.org/10.1175/MWR3276.1.

——, ——, ——, ——, and ——, 2007b: Dual-Doppler analysis of winds and vorticity budget terms near a tornado. *Mon. Wea. Rev.*, **135**, 2392–2405, https://doi.org/10.1175/MWR3404.1.

——, P. Robinson, C. Alexander, and Y. Richardson, 2007c: Low-level winds in tornadoes and potential catastrophic tornado impacts in urban areas. *Bull. Amer. Meteor. Soc.*, **88**, 31–46, https://doi.org/10.1175/BAMS-88-1-31.

——, K. Kosiba, P. Markowski, Y. Richardson, D. Dowell, and P. Robinson, 2010: Finescale single- and dual-Doppler analysis of tornado intensification, maintenance, and dissipation in the Orleans, Nebraska, supercell. *Mon. Wea. Rev.*, **138**, 4439–4455, https://doi.org/10.1175/2010MWR3330.1.

——, D. Dowell, Y. Richardson, P. Markowski, E. Rasmussen, D. Burgess, L. Wicker, and H. B. Bluestein, 2012: The second Verification of the Origins of Rotation in Tornadoes Experiment: VORTEX2. *Bull. Amer. Meteor. Soc.*, **93**, 1147–1170, https://doi.org/10.1175/BAMS-D-11-00010.1.

——, K. Kosiba, and P. Robinson, 2013a: In situ, Doppler radar, and video observations of the interior structure of a tornado and the wind–damage relationship. *Bull. Amer. Meteor. Soc.*, **94**, 835–846, https://doi.org/10.1175/BAMS-D-12-00114.1.

——, ——, ——, and F. J. Masters, 2013b: Fine-scale dual-Doppler and in-situ observations of the boundary layer in Hurricane Isaac. *36th Conf. on Radar Meteorology*, Breckenridge, CO, Amer. Meteor. Soc., 182, https://ams.confex.com/ams/36Radar/webprogram/Paper229319.html.

——, ——, ——, and T. Marshall, 2014: The role of multiple vortex tornado structure in causing storm researcher fatalities. *Bull. Amer. Meteor. Soc.*, **95**, 31–45, https://doi.org/10.1175/BAMS-D-13-00221.1.

——, and Coauthors, 2016: Very fine-scale Dual-Doppler and in-situ analysis of a strong tornado. *28th Conf. on Severe Local Storms*, Portland, OR, Amer. Meteor. Soc., 4.3, https://ams.confex.com/ams/28SLS/webprogram/Paper302005.html.

——, K. A. Kosiba, T. White, and P. Robinson, 2021: Supercell tornadoes are much stronger and wider than damage-based ratings indicate. *Proc. Natl. Acad. Sci. USA*, **118**, e2021535118, https://doi.org/10.1073/pnas.2021535118.

Ziegler, C. L., M. S. Buban, and E. N. Rasmussen, 2007: A Lagrangian objective analysis technique for assimilating in-situ observations with multiple-radar-derived airflow. *Mon. Wea. Rev.*, **135**, 2417–2442, https://doi.org/10.1175/MWR3396.1.

Unauthenticated | Downloaded 02/01/24 06:03 PM UTC